

# Global distribution and interannual variations of mesospheric and lower thermospheric neutral wind diurnal tide:

## 2. Nonmigrating tide

Q. Wu,<sup>1,2</sup> D. A. Ortland,<sup>3</sup> T. L. Killeen,<sup>1</sup> R. G. Roble,<sup>1</sup> M. E. Hagan,<sup>1</sup> H.-L. Liu,<sup>1</sup> S. C. Solomon,<sup>1</sup> Jiyao Xu,<sup>2</sup> W. R. Skinner,<sup>4</sup> and R. J. Niecejewski<sup>4</sup>

Received 14 May 2007; revised 6 January 2008; accepted 24 January 2008; published 17 May 2008.

[1] On the basis of the TIDI mesospheric and lower thermospheric neutral wind observations from 2002 (March) to 2007 (June), we analyze the interannual variations of nonmigrating diurnal tides from eastward zonal wave number 3 (E3) to westward zonal wave number 3 (W3). We focus on possible QBO-related variations in these nonmigrating diurnal tide components. We found: (1) a strong reverse QBO effect on the W2 meridional diurnal tide in the September equinox and the December solstice, which suggests a W2 source of nonlinear interaction between planetary wave 1 and the migrating diurnal tide; (2) the QBO effect on the peak height during the June solstice on the E3 zonal diurnal tide; (3) several nonmigrating tide components (E3, E2, E1, W3 meridional, and W3 zonal) with similar eastward phase QBO enhancement during the March equinox to the migrating diurnal tide, although to a lesser degree from 2002 to 2005; (4) the QBO effects, in some cases, during 2006 and 2007 are either less or opposite those observed between 2002 and 2005.

**Citation:** Wu, Q., D. A. Ortland, T. L. Killeen, R. G. Roble, M. E. Hagan, H.-L. Liu, S. C. Solomon, J. Xu, W. R. Skinner, and R. J. Niecejewski (2008), Global distribution and interannual variations of mesospheric and lower thermospheric neutral wind diurnal tide: 2. Nonmigrating tide, *J. Geophys. Res.*, 113, A05309, doi:10.1029/2007JA012543.

## 1. Introduction

[2] Besides the migrating diurnal tide, the nonmigrating diurnal tides are also significant at times. Nonmigrating diurnal tides are apparently caused by the following: latent heat release [e.g., Hagan and Forbes, 2002, 2003]; nonlinear interaction between the migrating tide and planetary wave [e.g., Hagan and Roble, 2001; Mayr et al., 2003; Lieberman et al., 2004; Mayr et al., 2005a, 2005b; Forbes et al., 1995; Teitelbaum and Vial, 1991]; and sea-land and orographic distributions [Tsuda and Kato, 1989; Kato et al., 1982]. Other sources are also suggested [Oberheide et al., 2002, 2006].

[3] On the basis of UARS HRDI observations, Talaat and Lieberman [1999], Forbes et al. [2003], and Huang and Reber [2004] examined the seasonal variations of various nonmigrating diurnal tides. Using TIDI observations, Oberheide et al. [2005a, 2006] studied the nonmigrating diurnal tides and compared the observations with TIME-GCM model results. Ground-based observations of the

nonmigrating tide are difficult and require multiple stations, often having only limited resolution for zonal wave numbers. To date, ground-based observations have been able to get only limited information about non-migrating tides and only at a few latitudes. When the nonmigrating tide becomes significant (e.g., at high latitudes), ground-based observations are able to provide good nonmigrating tide results [e.g., Murphy et al., 2003; Baumgaertner et al., 2006]. Recently, the MLT nonmigrating tide has been attributed to the longitudinal variations in the equatorial ionosphere anomaly [Sagawa et al., 2005; England et al., 2006a, 2006b; Immel et al., 2006]. Hence there is a renewed interest for a better understanding of the MLT nonmigrating tides.

[4] In general, there have been very few systematic nonmigrating tide observations, but modeling efforts have progressed in recent years [Hagan and Forbes, 2002, 2003; Grieger et al., 2004]. While we know more about the seasonal and latitudinal variations of the nonmigrating diurnal tide, very little has been shown about their interannual variabilities [Hagan et al., 2005; Oberheide et al., 2005b].

[5] In this paper, we focus on the interannual variation of the nonmigrating diurnal tide. This study is a continuation of the effort to examine the diurnal tides (migrating and nonmigrating) using TIDI observations. We should note that the TIDI instrument is ideal for the study of interannual variability because its latitudinal and local time sampling pattern is identical year after year. In our study, Wu et al.

<sup>1</sup>High Altitude Observatory, National Center for Atmospheric Research, Boulder, Colorado, USA.

<sup>2</sup>Key Laboratory for Space Weather, Center for Space Science and Applied Research, Chinese Academy of Sciences, Beijing, China.

<sup>3</sup>Northwest Research Associates, Bellevue, Washington, USA.

<sup>4</sup>Space Physics Research Laboratory, University of Michigan, Ann Arbor, Michigan, USA.

[2008, hereinafter referred to as Part I], we examined the migrating diurnal tide. For this study, we are particularly interested in the QBO effect as in Part I. The QBO effect on the migrating diurnal tide is strongest during the March equinox as shown in Part I. Therefore, we will primarily perform the interannual comparison of the March equinox diurnal tide amplitude. However, if other seasons also show possible QBO-related variation, we may examine these seasons instead. The data set and processing method are the same as those used in Part I. More details about the data set, stratospheric QBO wind conditions, and analysis method can be found in Part I.

[6] One of the intriguing problems is the way in which the nonmigrating tides react to the QBO. For the westward propagating nonmigrating tides, we would expect similar behaviors. For the eastward nonmigrating tides, we expect a different interaction with gravity waves because the momentum flux from the gravity waves is not isotropic. Hence, these results may shed light on how the gravity waves interact with the tides propagating in different directions. We do not include the NCAR TIME-GCM 1.2 annual results for this nonmigrating tide analysis because the TIME-GCM 1.2 annual runs were based on only GSWM migrating tide components at 10 hPa. We plan to perform new annual runs with nonmigrating tides at 10 hPa in the future.

[7] The paper is organized as follows. In section 2, we describe the nonmigrating diurnal tides of various modes in March equinox meridional and zonal winds during the six years from 2002 to 2007, based on the TIDI observations. Other seasons will be examined instead, if a strong QBO effect is found. We discuss the results in section 3 and summarize our findings in section 4.

## 2. TIDI Observation of Nonmigrating Diurnal Tide in Neutral Winds

[8] In past observations [e.g., *Forbes et al.*, 2003], the diurnal tide was found to have several prominent nonmigrating components. We limited our analysis to components from E3 to W3. Components beyond zonal wave number 3 are usually very small and not included in the discussion. For each nonmigrating diurnal tide component, we will start with the latitudinal and daily variations at 95 km; then, we will show the most QBO-affected seasons with a latitude and vertical variation plot.

### 2.1. Eastward Zonal Wave Number 3 (E3)

[9] Figure 1 shows the E3 in meridional winds at 95 km for the 6-year period (2002–2007). The E3 meridional tide is limited to the region near the equator. The amplitudes tend to peak during March and September equinoxes. Since the amplitude at 95 km gives no obvious QBO effect, we examine the amplitude profiles during the March equinox when the migrating diurnal tide shows the largest QBO effect. Figure 2 plots the E3 meridional amplitude vertical profiles during March equinox. Slightly stronger amplitudes were observed during the eastward phase of the stratospheric QBO years of 2002 and 2004. However, there appears to be a reversal in 2006 and 2007, with the amplitude in 2007 being larger than that in 2006.

[10] Figure 3 is for the zonal wind E3 amplitude. The large zonal wind E3 amplitude is also limited to the low latitudes, but the region is wider than that of the meridional winds. The maximum amplitude occurs between the June solstice and September equinox, and the amplitude is stronger during the eastward phase of the stratospheric QBO (2002, 2004, and 2006). To examine the amplitude change more closely, we plot the amplitude profiles of the September equinox in Figure 4. There is no clear peak amplitude difference between the eastward and westward phase of the QBO. There is a small difference in altitude of the E3 active region. During the eastward phase of the QBO (2002, 2004, and 2006), the region appears to be lower in altitude. Consequently, the 95 km amplitudes show an increase for the 2002, 2004, and 2006 June solstice and September equinox (Figure 3).

### 2.2. Eastward Zonal Wave Number 2 (E2)

[11] The meridional diurnal E2 component at 95 km is much weaker than that of the E3 in general (Figure 5) and is centered near 10°S. No clear QBO effect can be seen. Figure 6 shows the E2 vertical profiles during the March equinox. In this plot, we can see enhancement during the eastward phase of the stratospheric QBO (2002, 2004, and 2006). The meridional E2 amplitude during these 3 years (2002, 2004, and 2006) peaked at 10°S. We should also note that in 2007 the meridional E2 component is not weak. There is a much smaller contrast between the 2006 and 2007 results.

[12] Figure 7 shows E2 in the zonal winds at 95 km. There is a slight increase in amplitude in the December solstice at 50°S during the westward phase of the QBO (2003 and 2005). Figure 8 illustrates the vertical profiles of the E2 zonal amplitude during the December solstice. A narrow region of the enhanced amplitude can be seen during the westward phase of the stratospheric QBO (2003 and 2005). Again, the zonal E2 amplitude in 2006 near 50°S is also slightly enhanced.

### 2.3. Eastward Zonal Wave Number 1 (E1)

[13] The E1 meridional component peaks at 20°S most of the time (Figure 9). Two strong peaks appeared in the 2002 and 2003 September equinoxes. There is a small increase in the March equinoxes of 2002 and 2004. The vertical profile of the meridional amplitude for the March equinox shows a small increase around 20°S for the eastward stratospheric QBO phase (Figure 10). In the case of 2006 and 2007, the amplitude in 2006 is still larger than that in 2007. However, the meridional E1 amplitude in 2007 is the second largest appearing in all years. The E1 in the zonal winds at 95 km is shown in Figure 11. We see no consistent seasonal pattern. The vertical profiles during the March equinox (not shown) also have no identifiable features.

### 2.4. Stationary Zonal Wave Number 0 (S0)

[14] The meridional wind S0 component has two tracks at 20°S and 20°N (Figure 12). The amplitude has a tendency to maximize near day 250 (7 September). The maximum amplitude in the September equinox tends to be larger at 20°N (between days 200, 18 July and 300, 27 October) for the westward phase of the QBO, whereas the maximum at

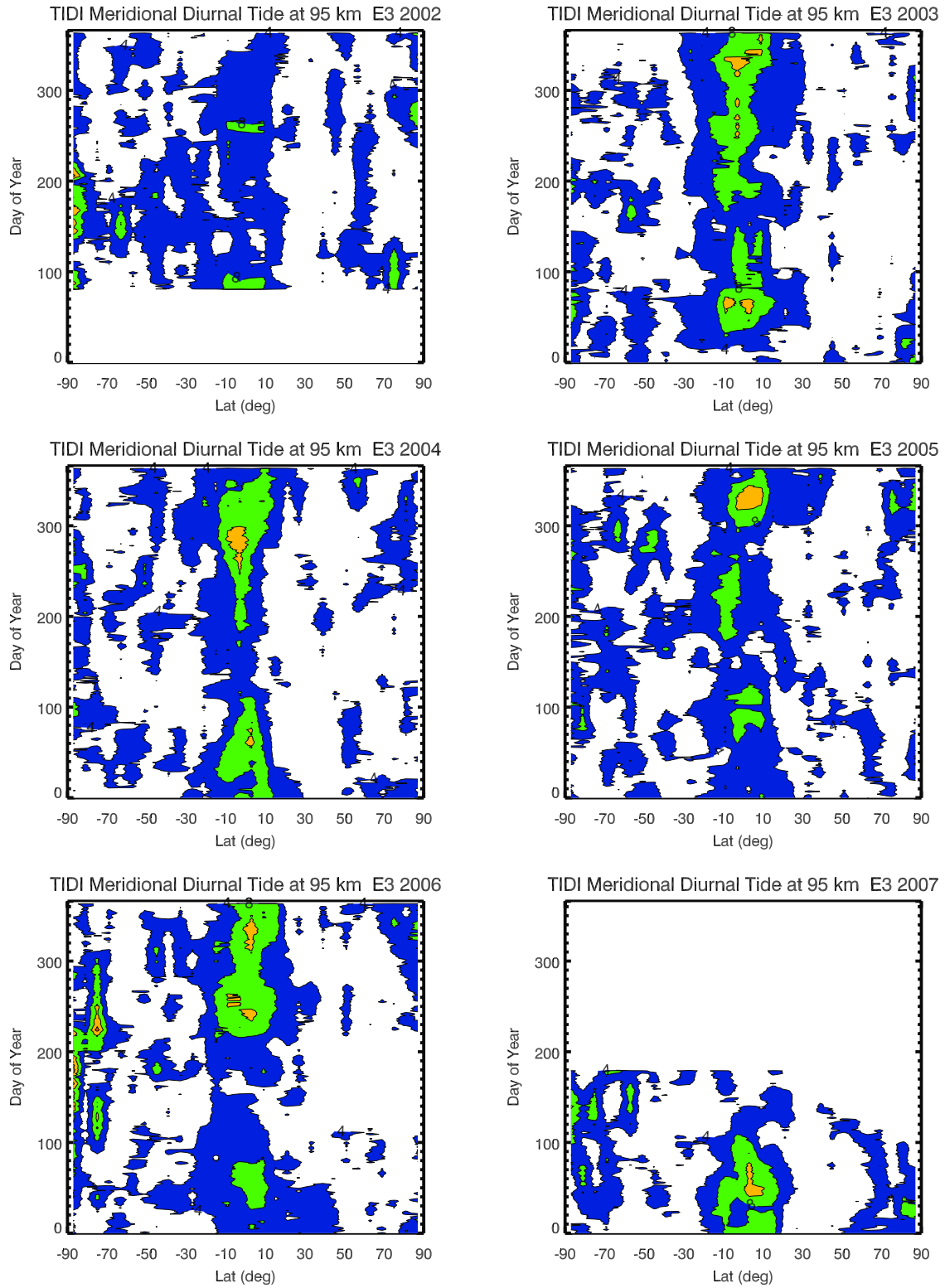


**Figure 1.** Diurnal E3 in meridional winds at 95 km. The plot is based on analysis with a 60-d sliding window; the date in vertical direction marks the center of the 60-d window. The left side is for the eastward phase of the stratosphere QBO (2002, 2004, and 2006), whereas the right side is for the westward phase. The contour level step is 4 m/s.

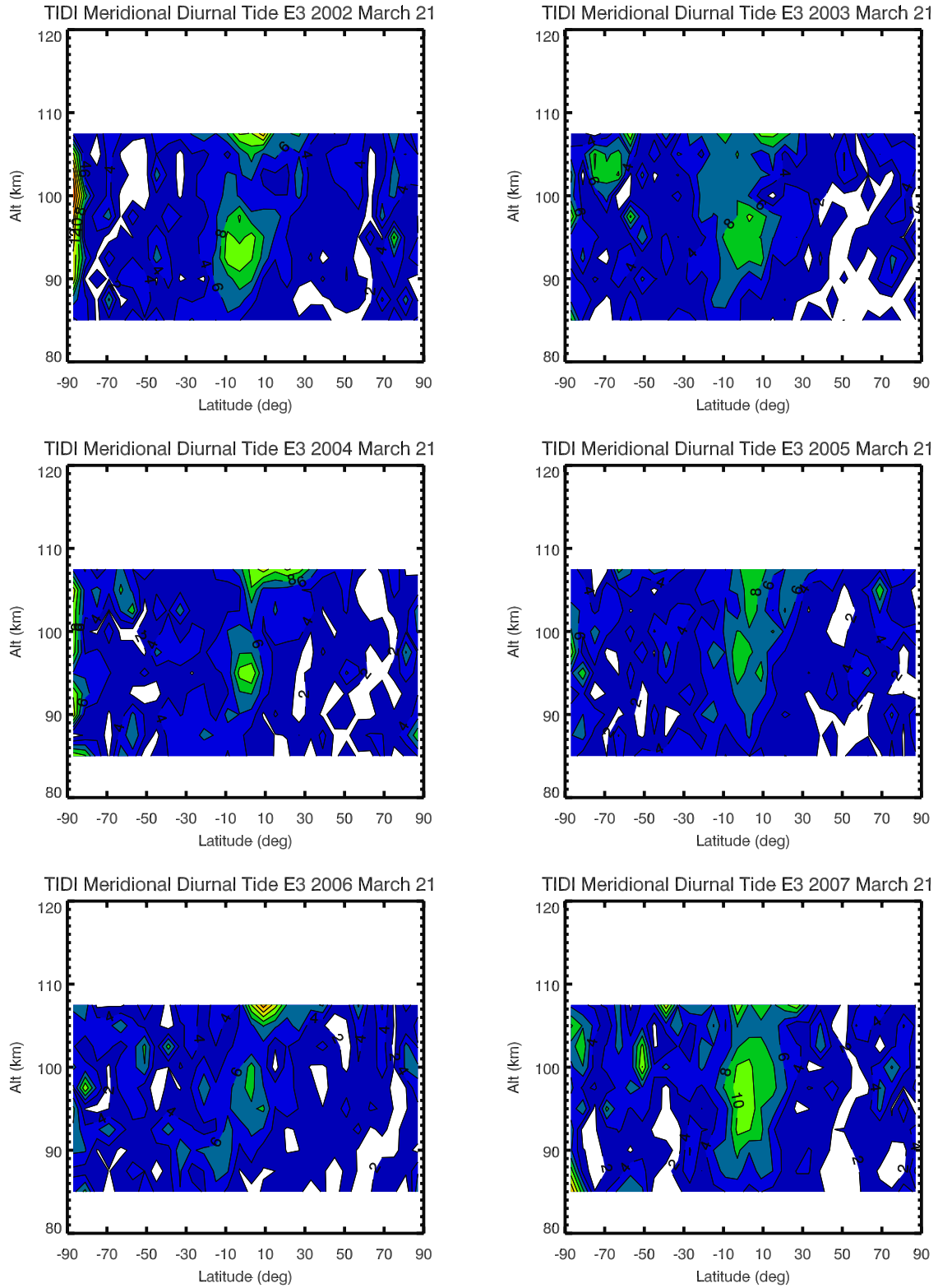


**Figure 2.** Diurnal E3 in meridional winds during the March equinox. The latitudinal and vertical variations of the meridional E3 diurnal tide amplitude during the March equinox. Again the left side is for the eastward phase of the stratosphere QBO (2002, 2004, and 2006) and the westward phase is on the right side (2003, 2005, and 2007). The contour level step is 2 m/s.



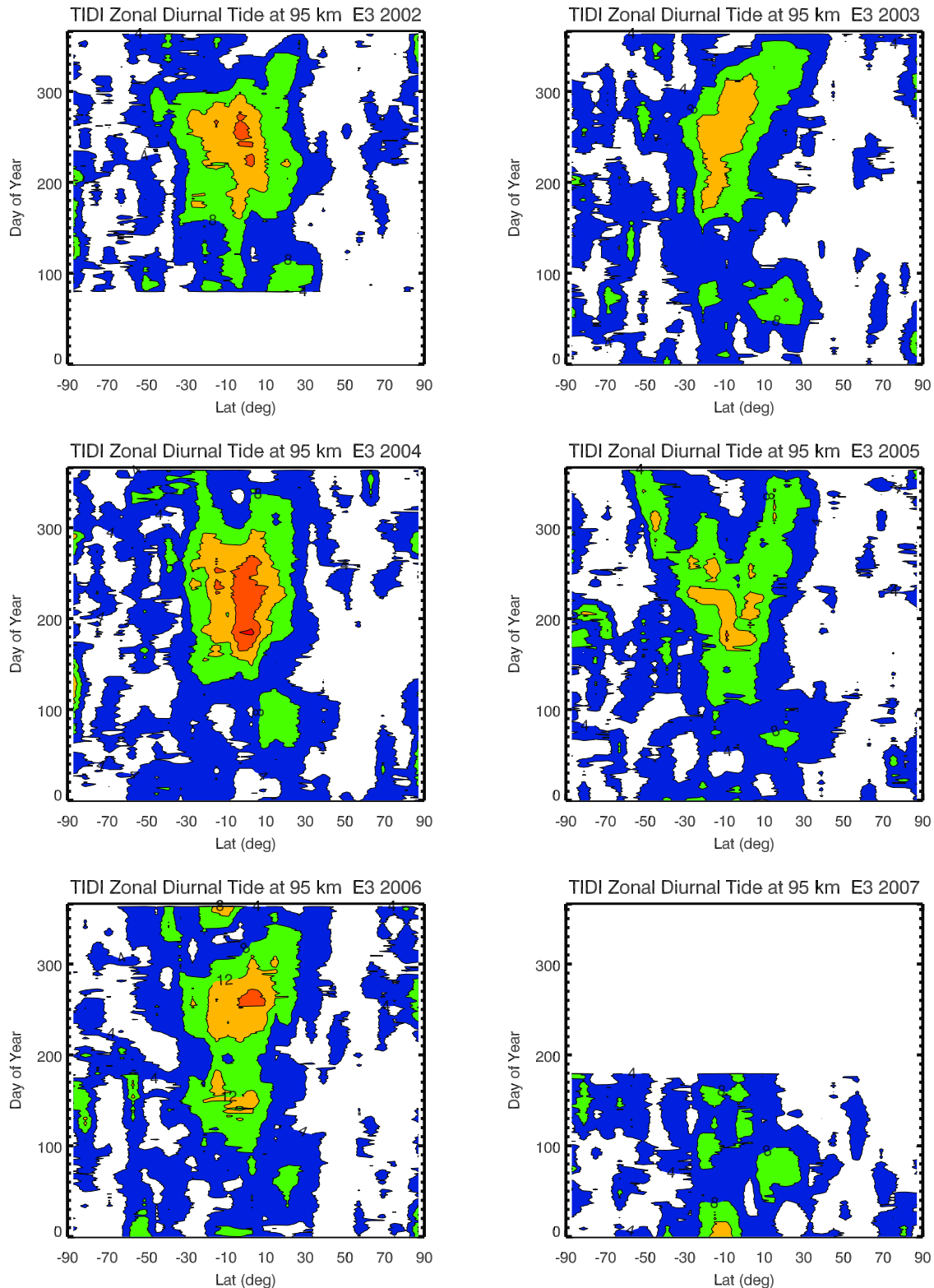


**Figure 3.** Diurnal E3 in zonal winds at 95 km. Same as Figure 1 for E3 in meridional winds.

20°S (near day 200, 18 July) shows no such regularity. Figure 13 shows the March equinox vertical profiles, which reveal no apparent QBO-related changes. The zonal wind S0 component at 95 km does not have a well-defined pattern (Figure 14). Most of its activities are in the southern hemisphere near 50°S.

## 2.5. Westward Zonal Wave Number 2 (W2)

[15] The meridional wind W2 component has a well-defined pattern with amplitude crests at 20°S and 20°N (Figure 15). The amplitude has two peaks on days 230 (19 August) and 300 (27 October). The amplitude is quite significant, particularly in 2005, reaching  $\sim 30$  m/s. The

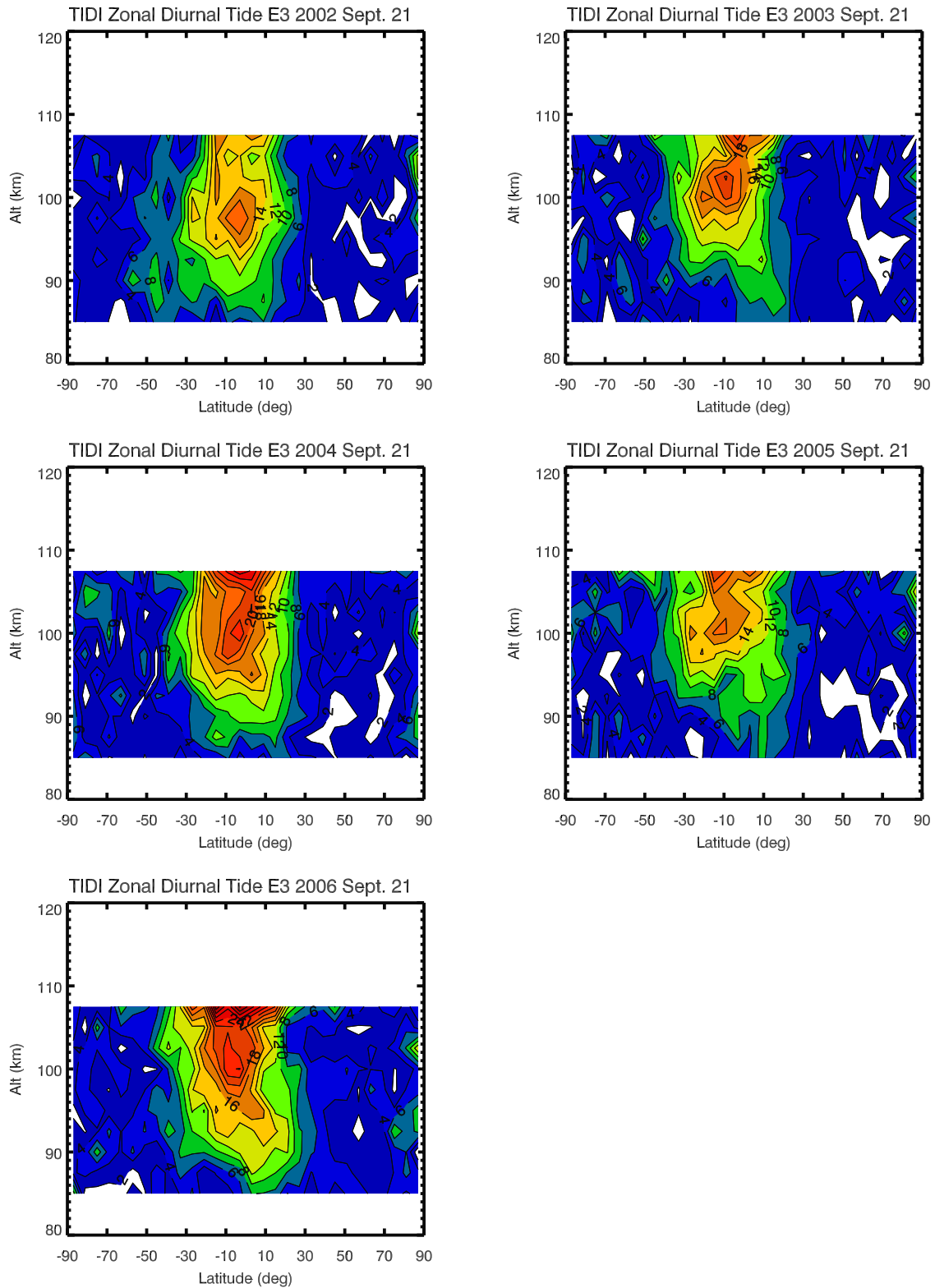


**Figure 4.** Diurnal E3 in zonal winds during the September equinox. Same as Figure 2 for E3 in zonal winds during the September equinox.

QBO effect is very pronounced, with larger amplitude in the September equinox and December solstice during the westward phase of the QBO (2003 and 2005). Strong interhemispheric differences are also seen. Figure 16 shows the

vertical and latitude variations of the September equinox meridional wind W2 amplitude. Stronger amplitude in 2003 and 2005 is quite apparent. The amplitude is also much stronger in the northern hemisphere at this time of the year

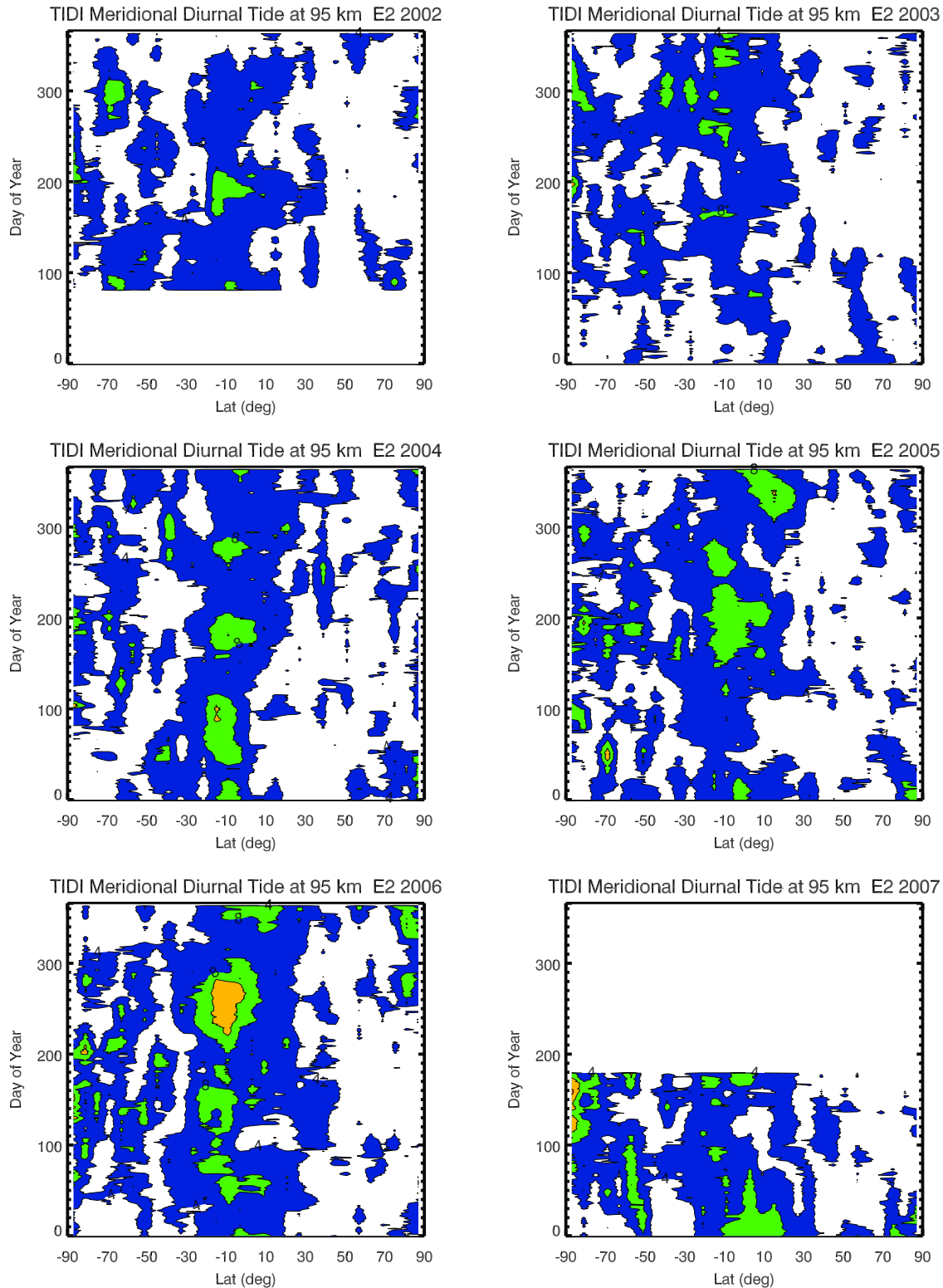


**Figure 5.** Diurnal E2 in meridional winds at 95 km. Same as Figure 1 for E2 in meridional winds.

than that in the southern hemisphere. For 2006, there is stronger amplitude in the southern hemisphere than in that in the northern hemisphere, which is different from all other years.

[16] Relative to the meridional winds, the zonal wind W2 component is much less well organized (Figure 17). At

30°N near day 300 (27 October) in 2003 and 2005, we see a small region of enhancement. At 53°S near day 200 (18 July), a persistent active region appeared in 2003, 2004, and 2005. Other active regions scattered across the southern hemisphere throughout the years.

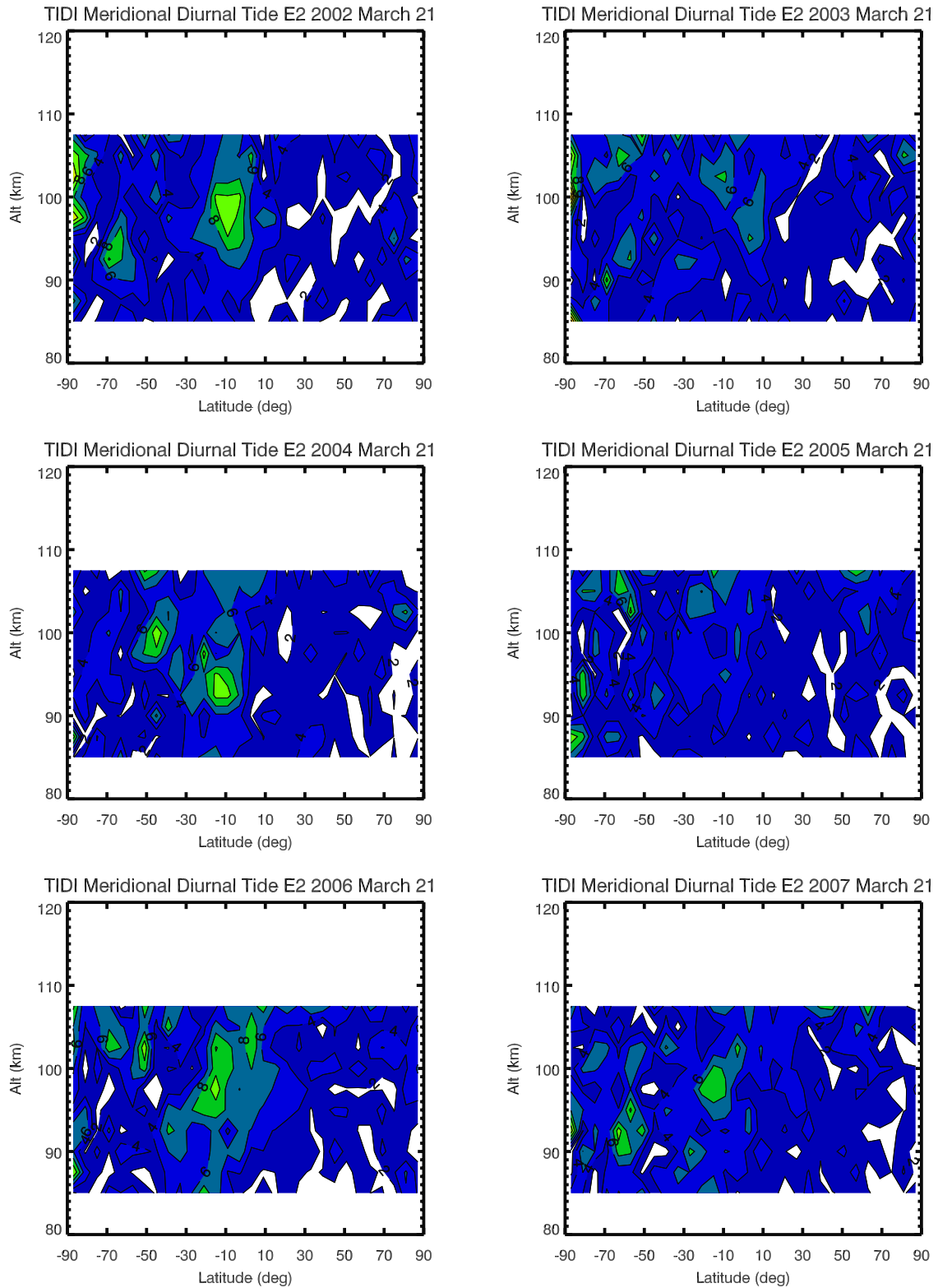


**Figure 6.** Diurnal E2 in meridional winds during the March equinox. Same as Figure 2 for E2 in meridional winds during the March equinox.

[17] Figure 18 shows the vertical profile of the zonal W2 amplitude in the September equinox. The two-peak structure at 30°N and 30°S is apparent for 2003 and 2005 and absent in 2002 and 2004. In 2006, the amplitude for

zonal W2 is also stronger in the southern hemisphere than any other years, although no 2007 data are available for comparison.



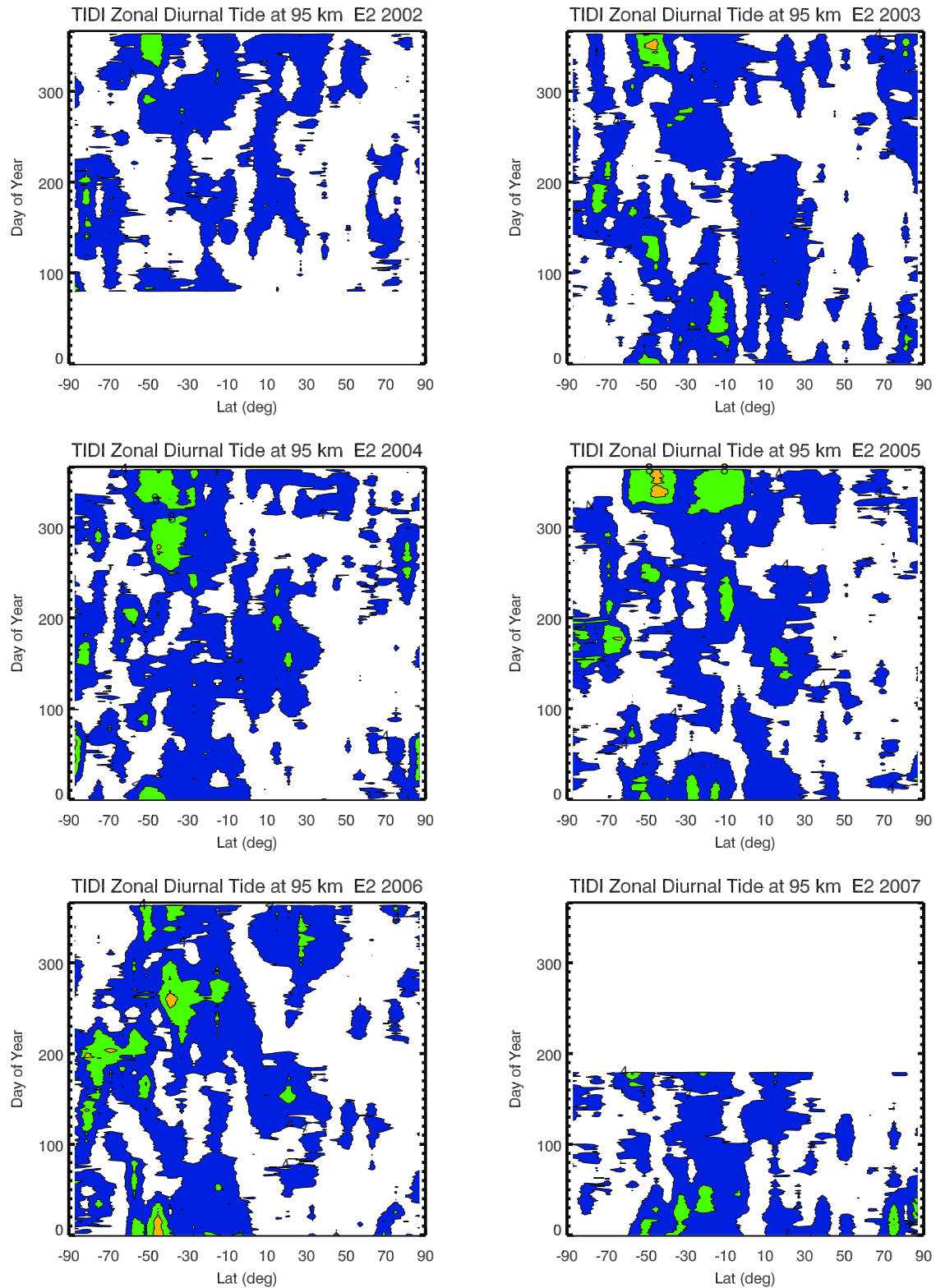


**Figure 7.** Diurnal E2 in zonal winds at 95 km. Same as Figure 1 for E2 in zonal winds.

## 2.6. Westward Zonal Wave Number 3 (W3)

[18] Although its amplitude is not strong, the meridional W3 component has a clear annual pattern with a peak at 20°S near day 260, 17 September (Figure 19). Less noticeable are the enhancements near day 80 (20 March) between

50°S and 10°S in 2002 and 2004. Figure 20 shows the vertical and latitudinal variations of the W3 during the March equinox. The enhancement is primarily between 50°S and 10°S during the eastward phase of the stratospheric QBO (2002, 2004, and 2006). The enhanced amplitude in

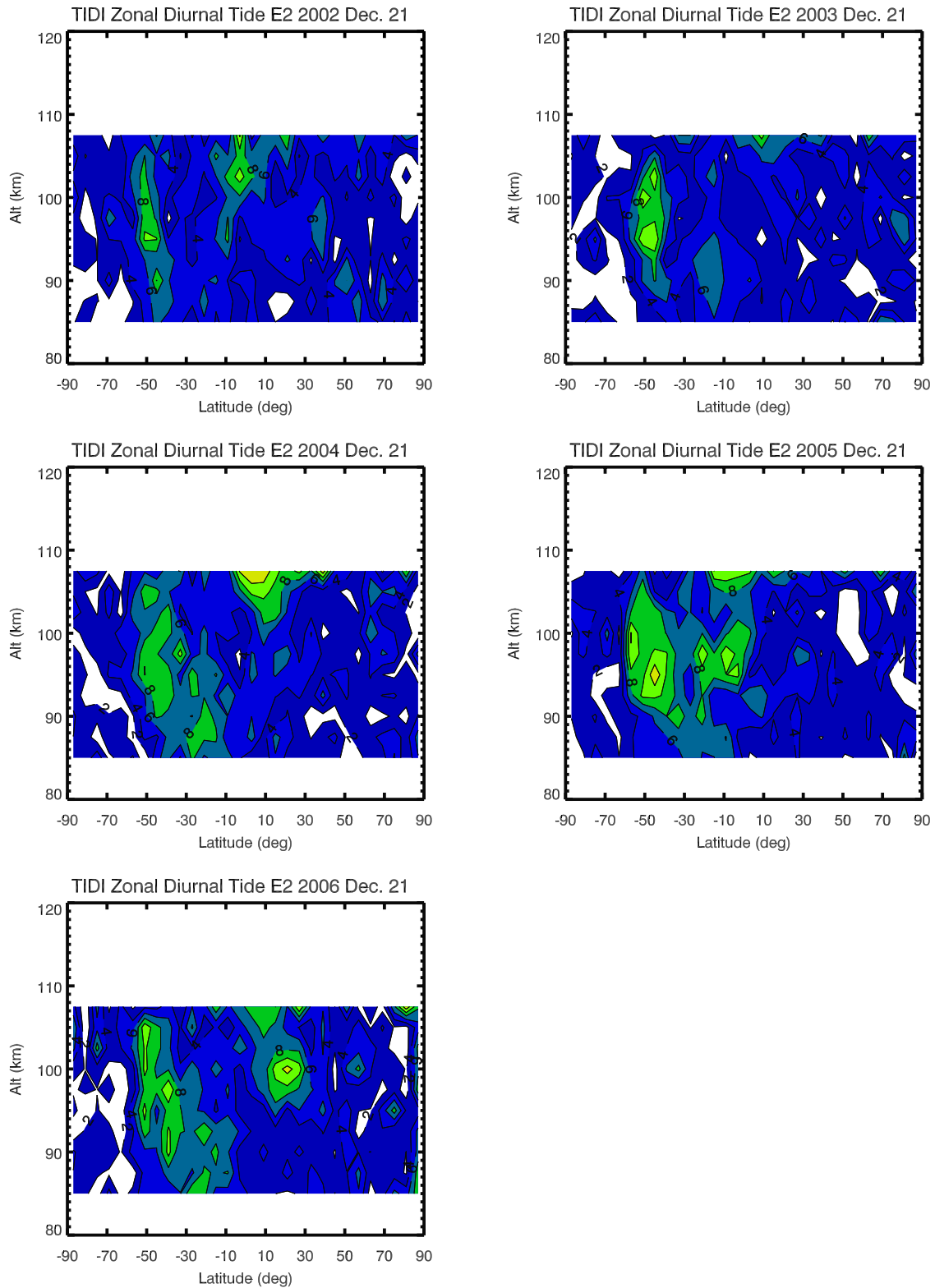


**Figure 8.** Diurnal E2 in zonal winds during the December solstice. Same as Figure 2 for E2 in zonal winds during the December solstice.

2007 again is not consistent with the trend in the other years.

[19] The zonal wind W3 component pattern is less clear at 95 km (Figure 21). Most active regions are in the southern hemisphere. Small enhancements are seen at 50°S near day

70 (10 March). The vertical and latitudinal variation plot for the March equinox shows an increase close to 50°S during the eastward phase of the QBO (in Figure 22). Enhanced amplitude in 2007 is observed again.

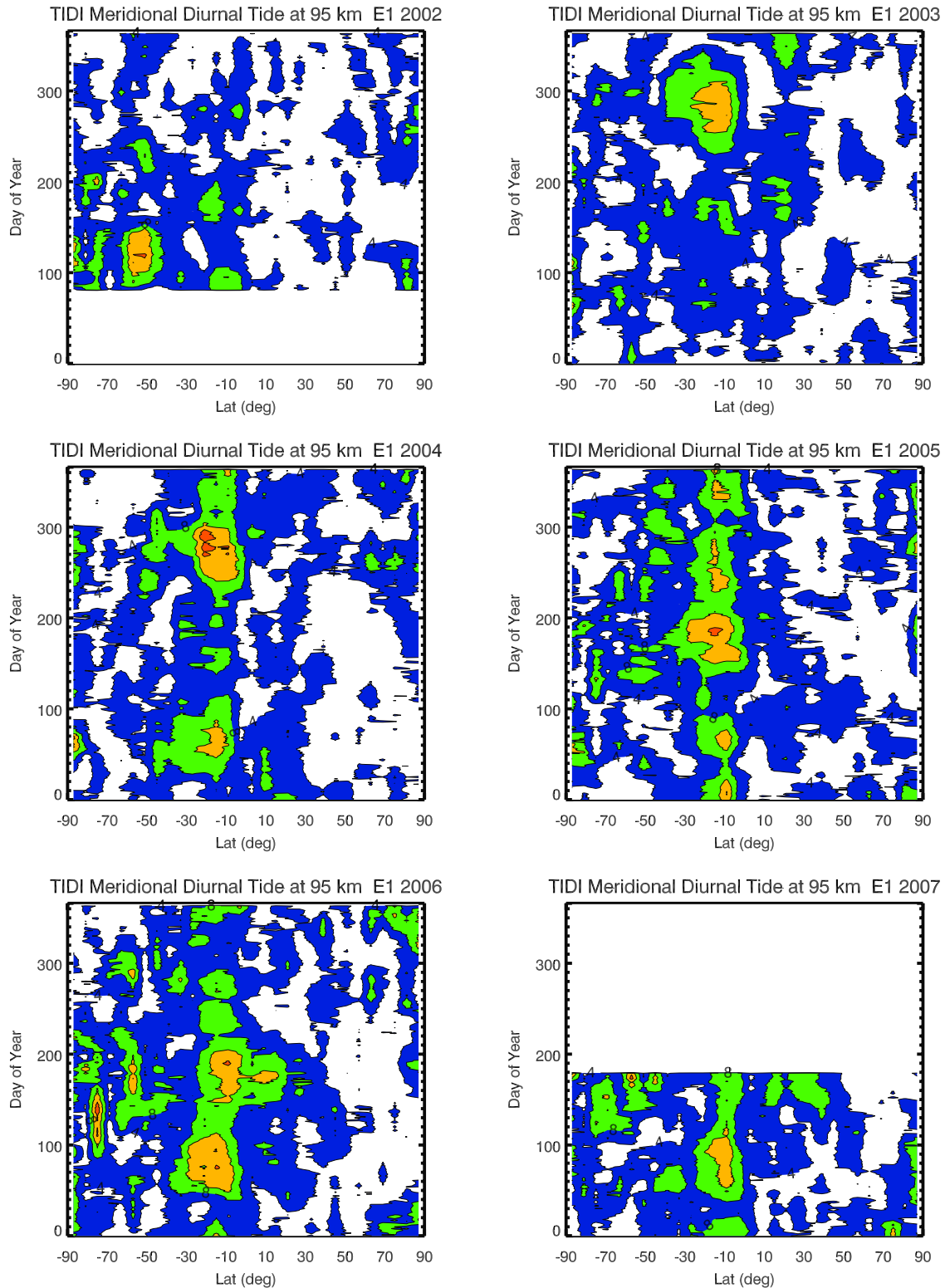


**Figure 9.** Diurnal E1 in meridional winds at 95 km. Same as Figure 1 for E1 in meridional winds.

[20] In order to have a comparison of all components, we plot all nonmigrating components from E3 to W3 at 20°N and at the equator for the meridional and zonal winds, respectively (Figure 23). The meridional wind W2 component at 20°N shows a strong correlation with the QBO (Figure 23a). A smaller correlation may exist for the S0

component. The QBO signal is weak for the other components at this latitude and altitude. That is not to say that other meridional nonmigrating diurnal tides are not affected by the QBO. The zonal E3 components show a strong QBO signal (Figure 23b), while at this particular latitude and altitude, others do not. Similarly, we should not assume a

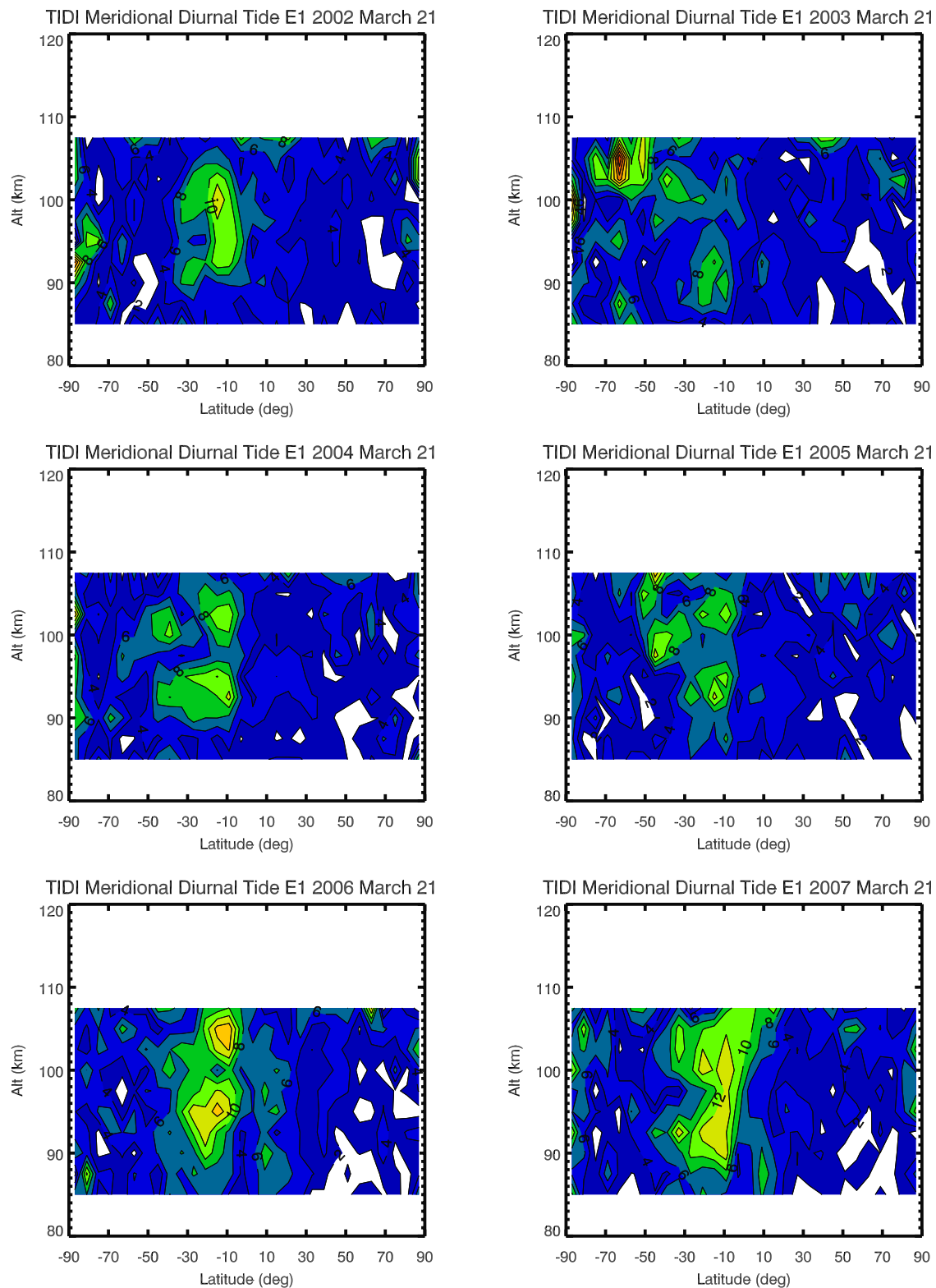


**Figure 10.** Diurnal E1 in meridional winds during the March equinox. Same as Figure 2 for E1 in meridional winds during the March equinox.



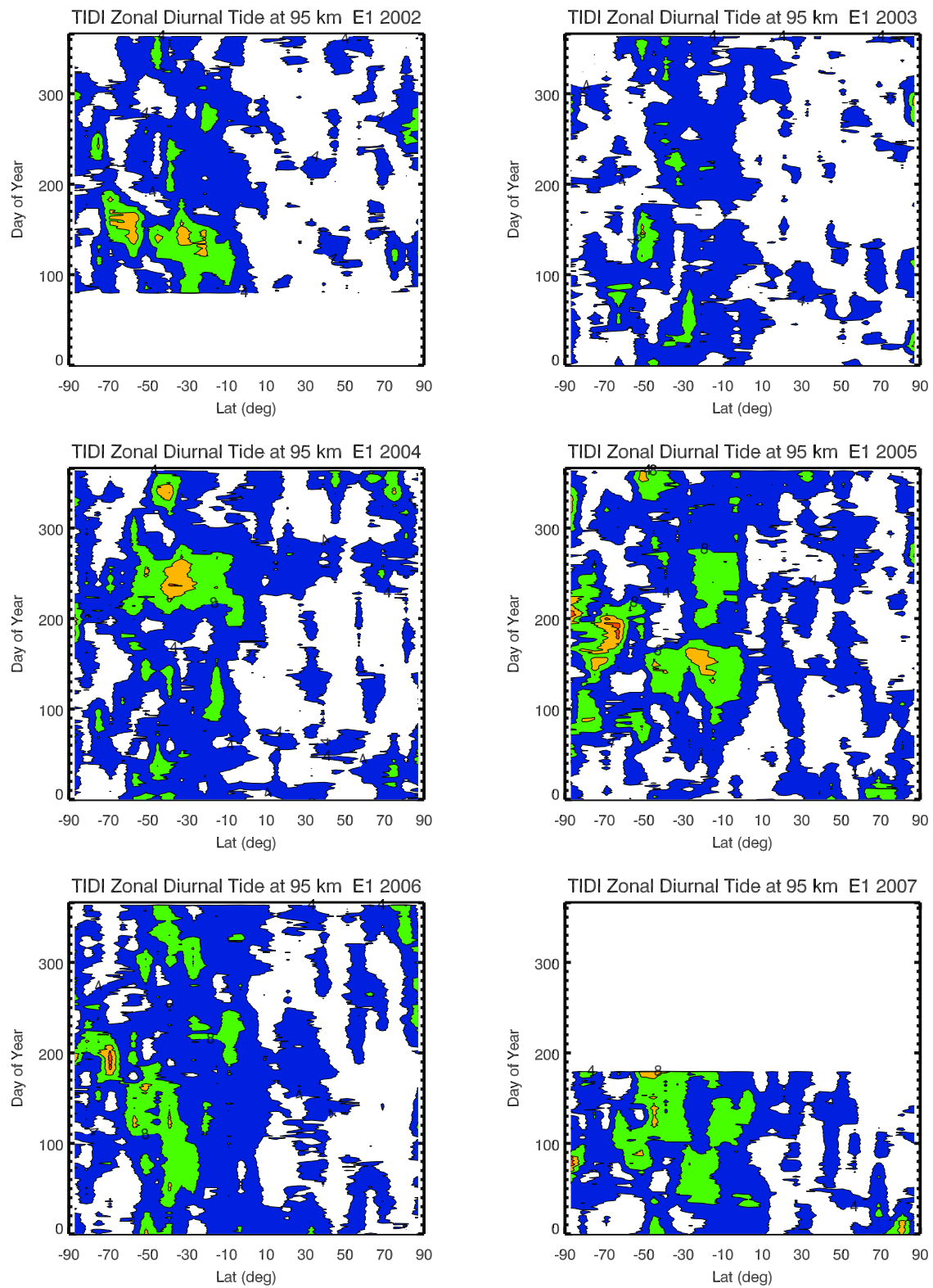


**Figure 11.** Diurnal E1 in zonal winds at 95 km. Same as Figure 1 for E1 in zonal winds.

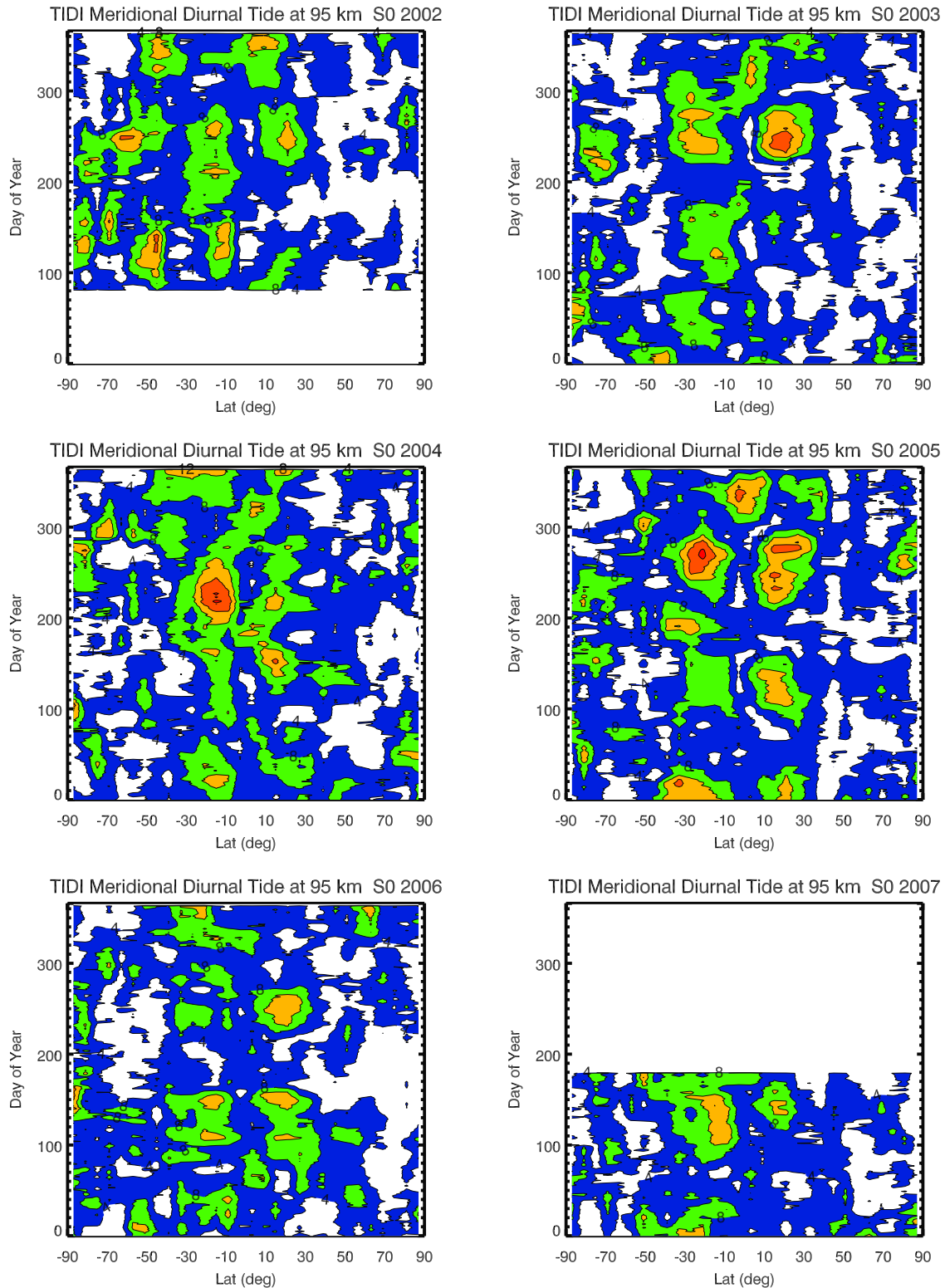


**Figure 12.** Diurnal S0 in meridional winds at 95 km. Same as Figure 1 for S0 in meridional winds.

lack of QBO-related signals in other zonal wind nonmigrating diurnal tides at other altitudes and latitudes.

### 3. Discussion

[21] There are not many systematic analyses of interannual variations of the diurnal nonmigrating tides. The

seasonal variations at 95 km for E3, S0, and W2 are very much consistent with those observed by *Oberheide et al.* [2006]. The TIDI instrument provides an opportunity with consistent and dedicated MLT neutral wind observations. Moreover, the TIDI coverage is identical year after year, making it ideal for interannual variability studies. The

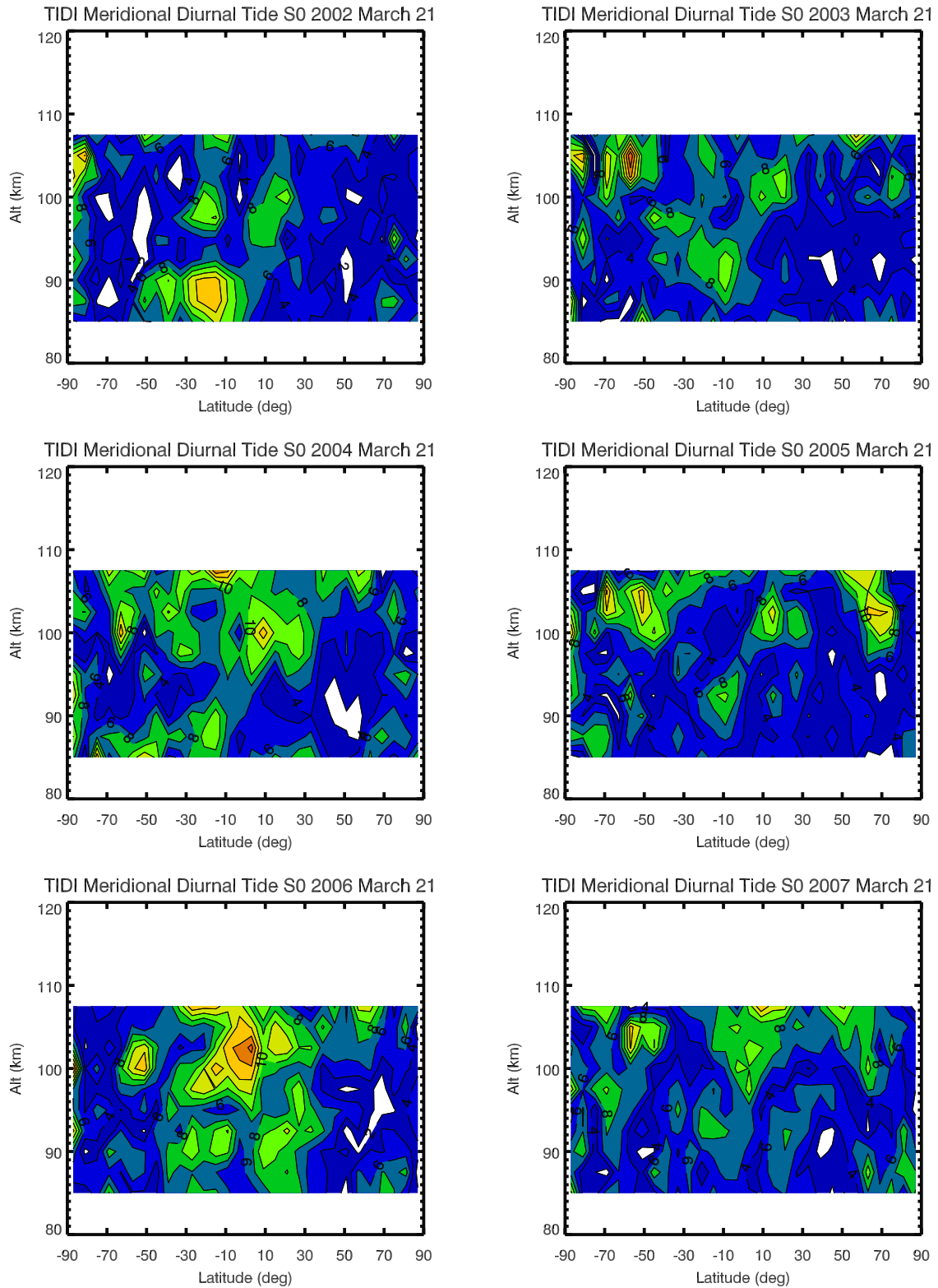


**Figure 13.** Diurnal S0 in meridional winds during the March equinox. Same as Figure 2 for S0 in meridional winds during the March equinox.

strongest reaction to the QBO is that of the meridional diurnal W2 during the September equinox. At that time, we see a reversed QBO on the meridional diurnal W2 with enhancement in the westward phase of the QBO. The QBO

effect on the meridional E3 is also noticeable in terms of peak altitude shift in the June solstice.

[22] Some changes are very subtle. For the S0 meridional wind component, we see changes in latitude and altitude of

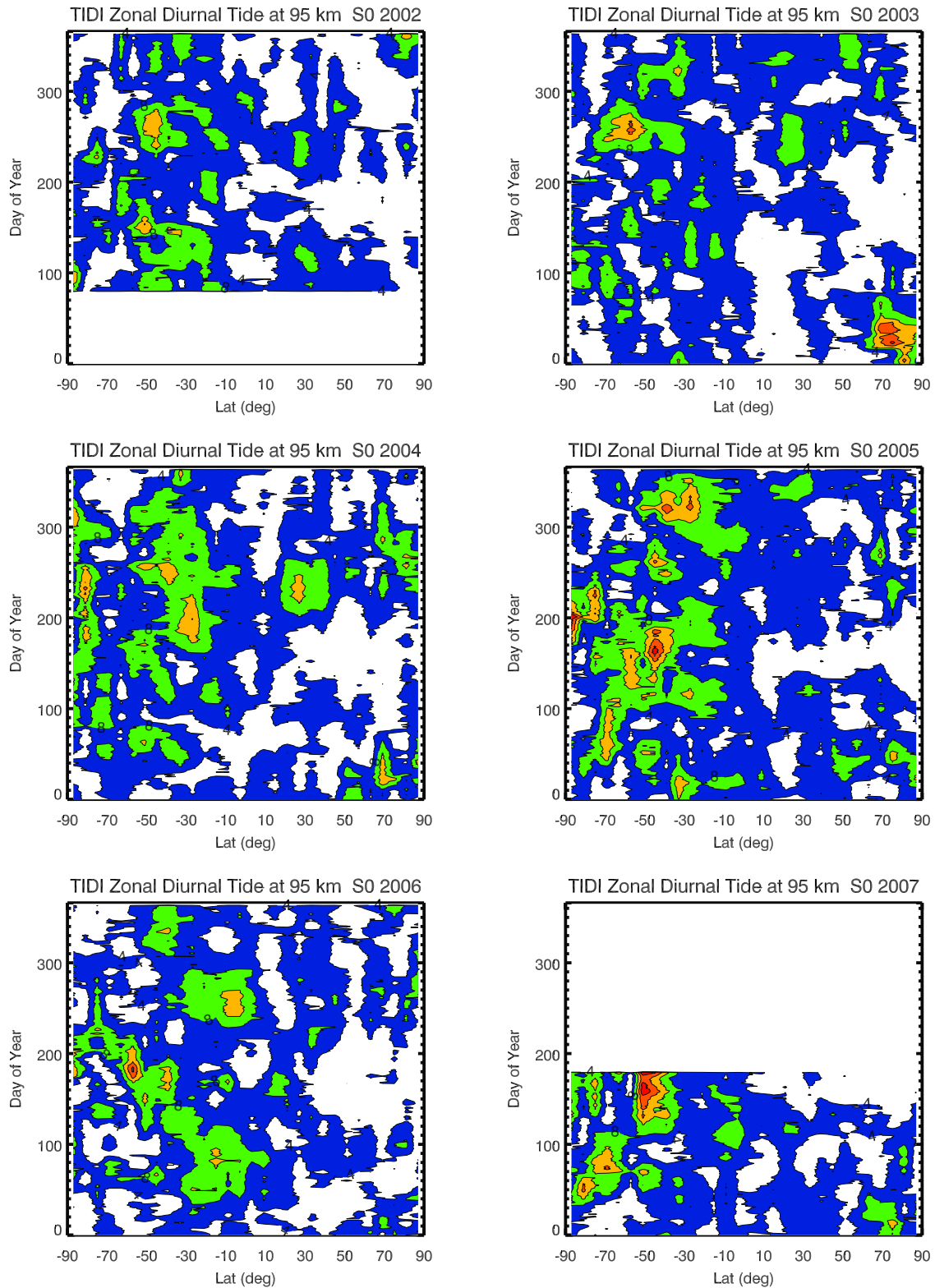


**Figure 14.** Diurnal S0 in zonal winds at 95 km. Same as Figure 1 for S0 in zonal winds.

the large amplitude during different phases of the QBO. Whether those changes are due to excitations of different modes is a question needs further studies.

[23] For most of the other components, we see a smaller enhancement in the March equinox during the eastward

phase of the QBO. Even for some eastward propagating components, we also see an increase in the eastward phase of the QBO. One would expect that the QBO affects tides through filtering of gravity waves. Such a mechanism would not be isotropic; gravity waves may interact with



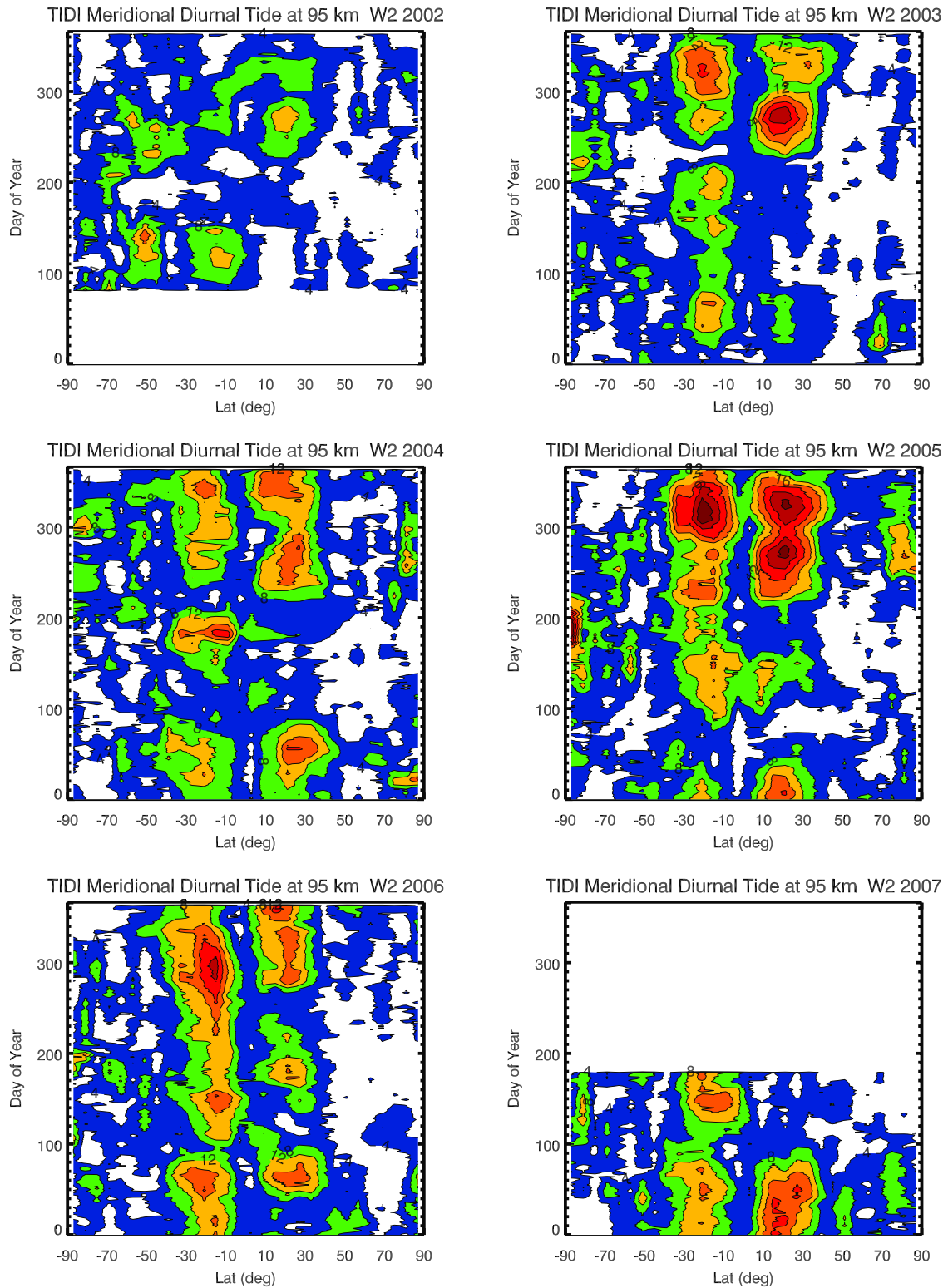


**Figure 15.** Diurnal W2 in meridional winds at 95 km. Same as Figure 1 for W2 in meridional winds.

nonmigrating tides propagating in the eastward direction differently compared to westward migrating diurnal tide. Yet we see a QBO modulation on these eastward propagating tides similar to the westward migrating tides. This result suggests that the nonmigrating diurnal tides may be related to the migrating tide. Although there have been in-depth

discussions about the nonlinear interaction between the migrating diurnal tide and a planetary waves causing the nonmigrating tides [e.g., *Mayr et al.*, 2005a, 2005b], such discussions have not extended to the eastward propagating nonmigrating diurnal tides. It is worth investigating the

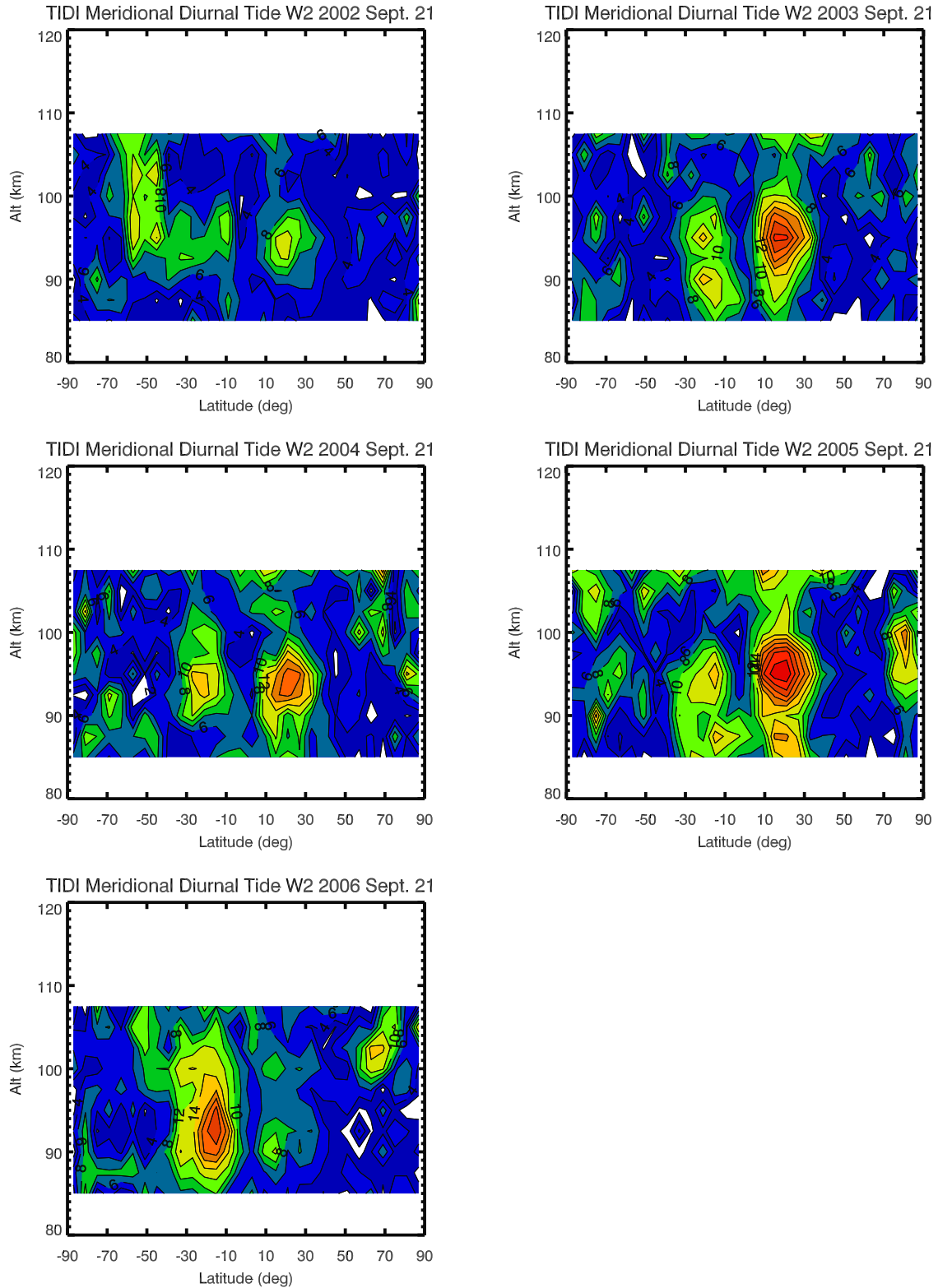


**Figure 16.** Diurnal W2 in meridional winds during the March equinox. Same as Figure 2 for W2 in meridional winds during the March equinox.

contribution to the eastward propagating nonmigrating diurnal tides from the migrating diurnal tide.

[24] The W2 component peaks in the September equinox and December solstice. The QBO modulation is reversed. If

we consider the W2 as the result of a nonlinear interaction between the migrating W1 and the planetary wave 1 as suggested by *Lieberman et al.* [2004], this reversed QBO modulation may then be traced to QBO modulation of the

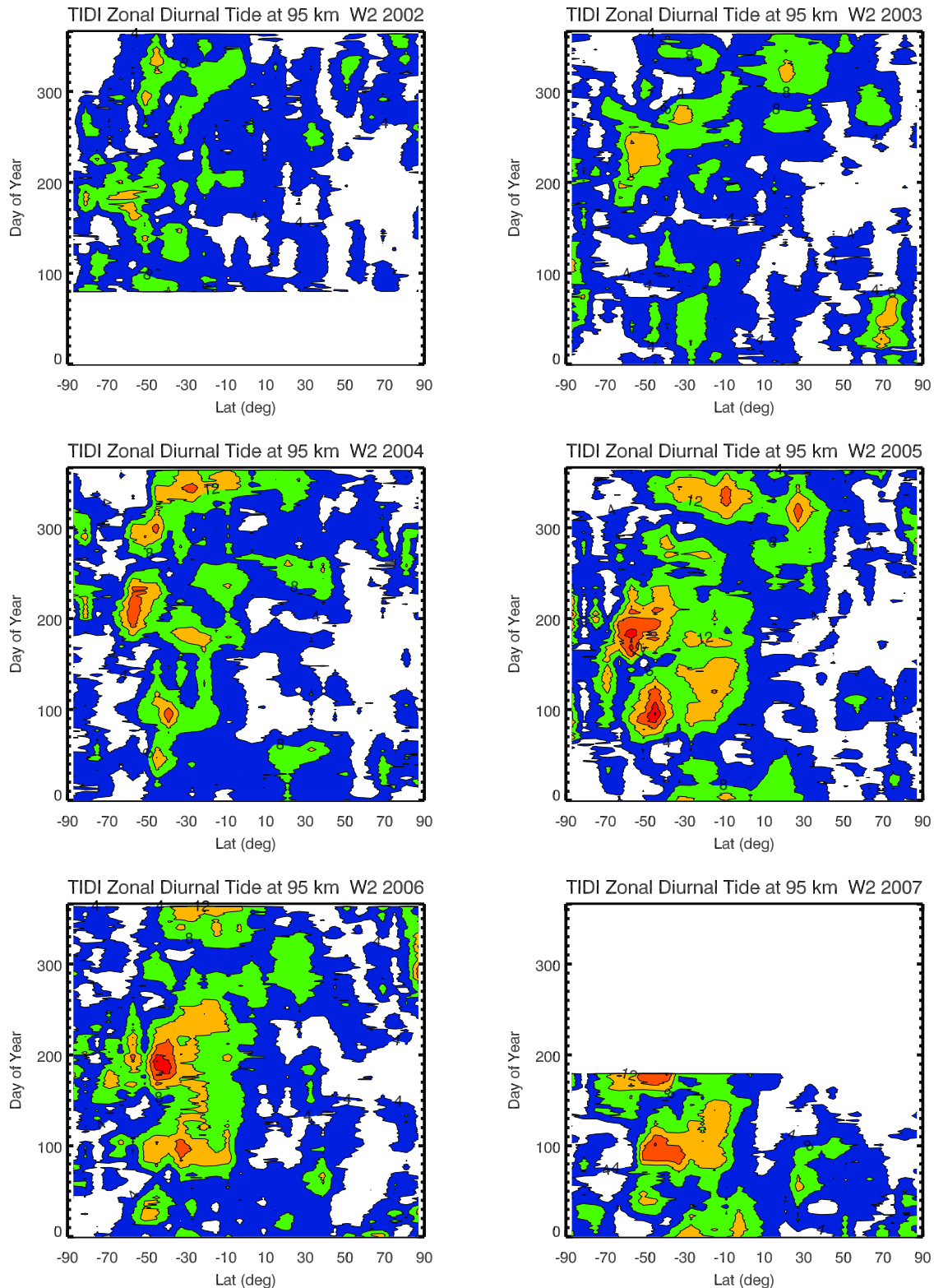


**Figure 17.** Diurnal W2 in zonal winds at 95 km. Same as Figure 1 for W2 in zonal winds.

planetary wave 1 in the stratosphere. *Hu and Tung* [2002] have noted such a reversed QBO modulation stratospheric planetary wave 1 during the December solstice. Therefore, our results lend more credence to the notion that the W2

diurnal tide is caused by the nonlinear interaction between the migrating W1 and the planetary wave 1.

[25] Beyond these variations possibly associated with the QBO, we have also seen large variations that apparently are not related to the QBO. More studies are needed to ascertain

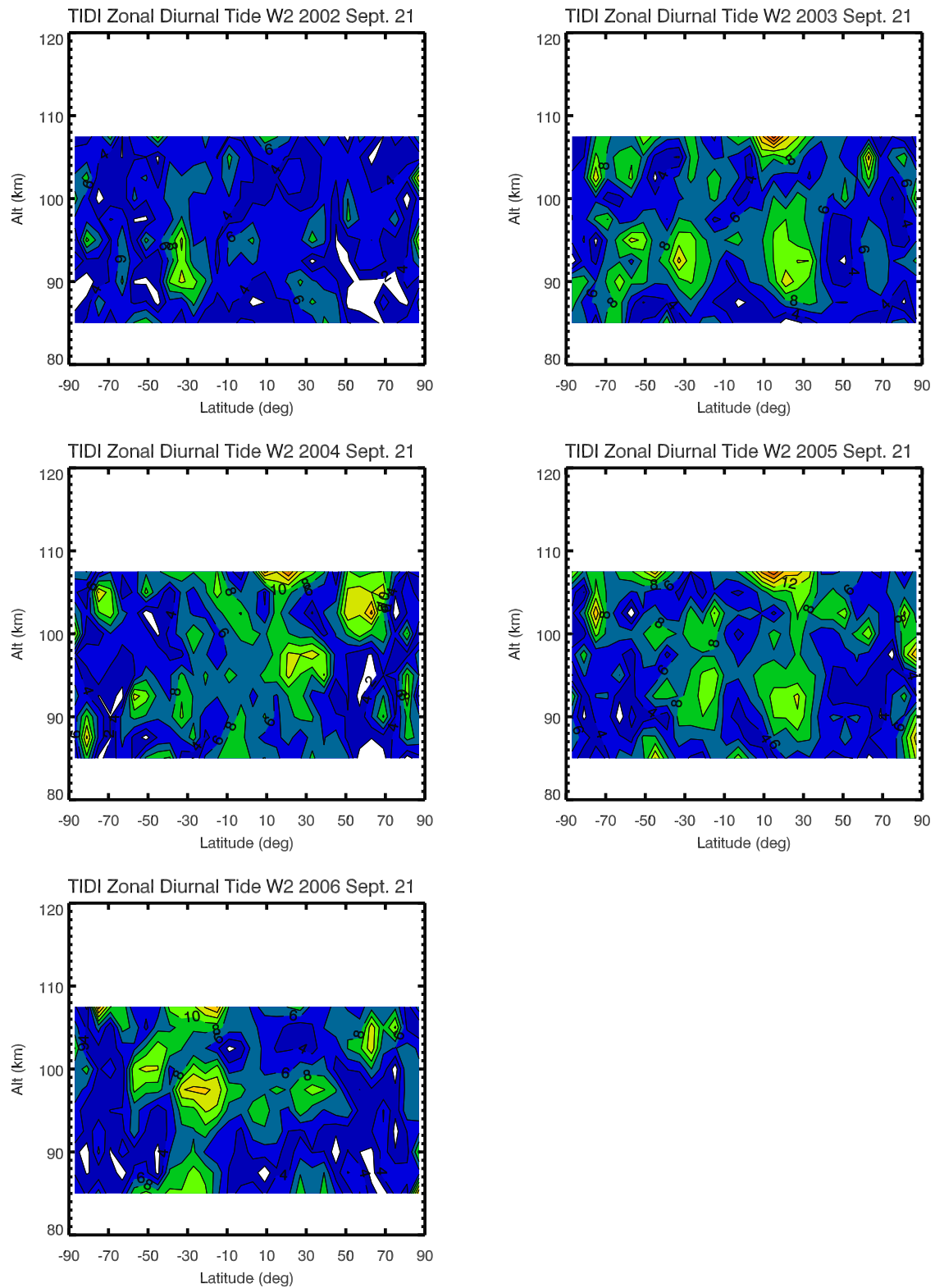


**Figure 18.** Diurnal W2 in zonal winds during the September equinox. Same at Figure 2 for W2 in zonal winds during the September equinox.



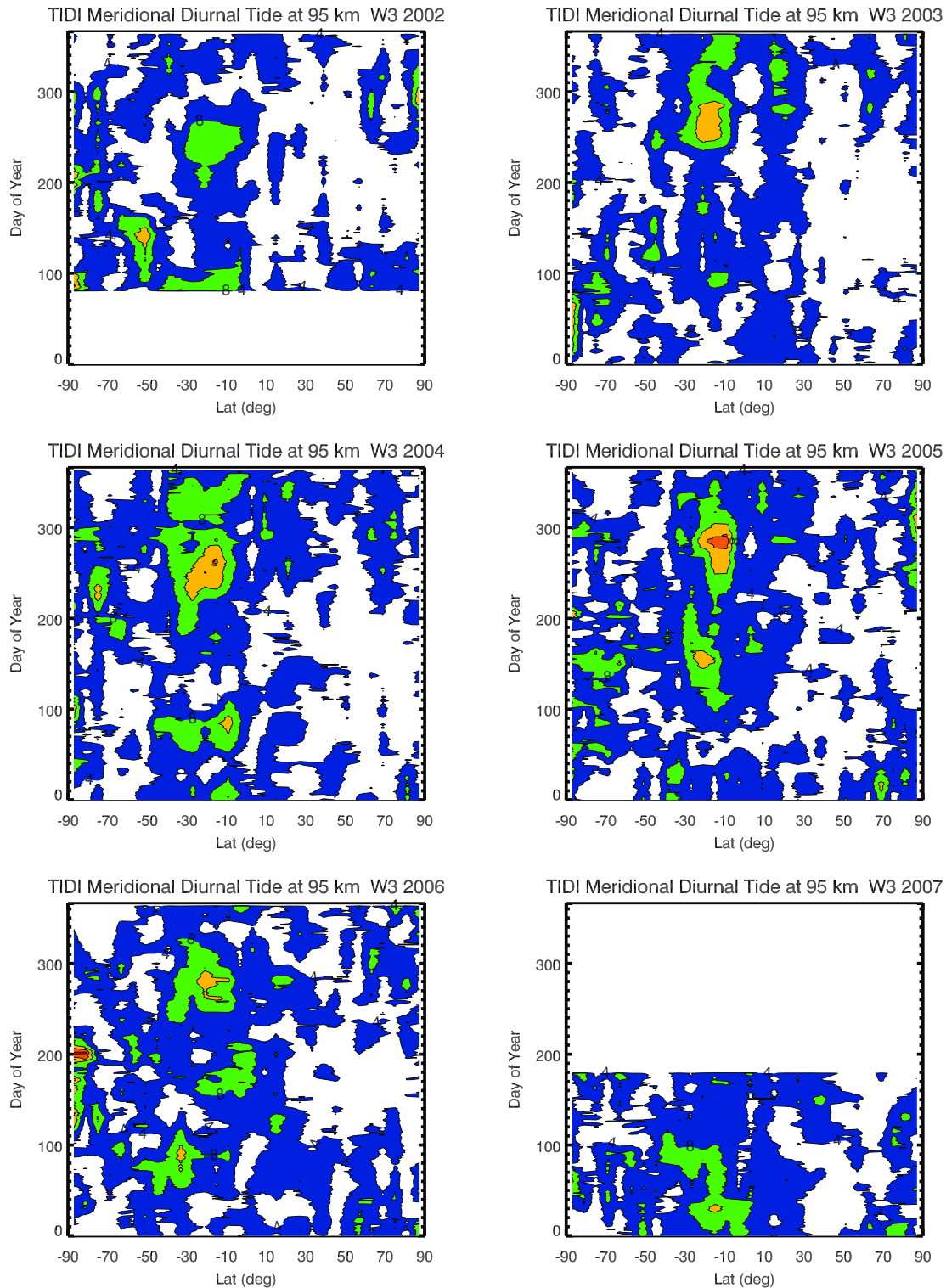


**Figure 19.** Diurnal W3 in meridional winds at 95 km. Same as Figure 1 for W3 in meridional winds.

the cause or causes for these variations. Also observed and requiring further study are large hemispheric asymmetries in tidal amplitudes.

#### 4. Summary

[26] Here, we have given only a brief overview of the interannual variation of the nonmigrating diurnal tide. Some

of nonmigrating diurnal tides show significant interannual variabilities: some may be QBO-related and some may not. We are far from understanding these variations at this point. Future studies with sophisticated models with proper QBO and stratospheric-mesospheric interactions are needed. In summary, we found (1) a strong reversed QBO effect on the W2 meridional diurnal tide in the September equinox and the December solstice, suggesting a source of nonlinear

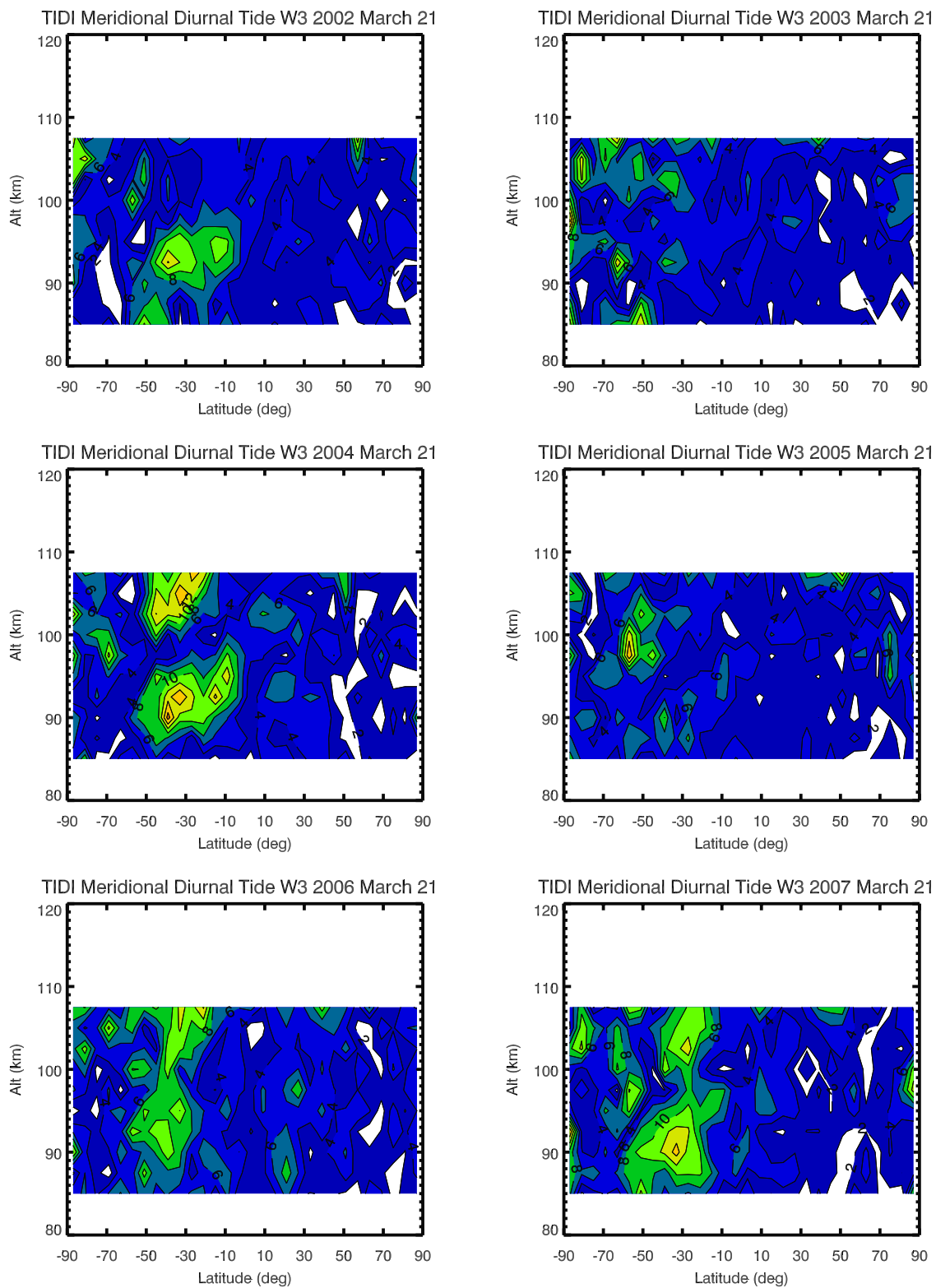


**Figure 20.** Diurnal W3 in meridional winds during the March equinox. Same as Figure 2 for W3 in meridional during the March equinox.

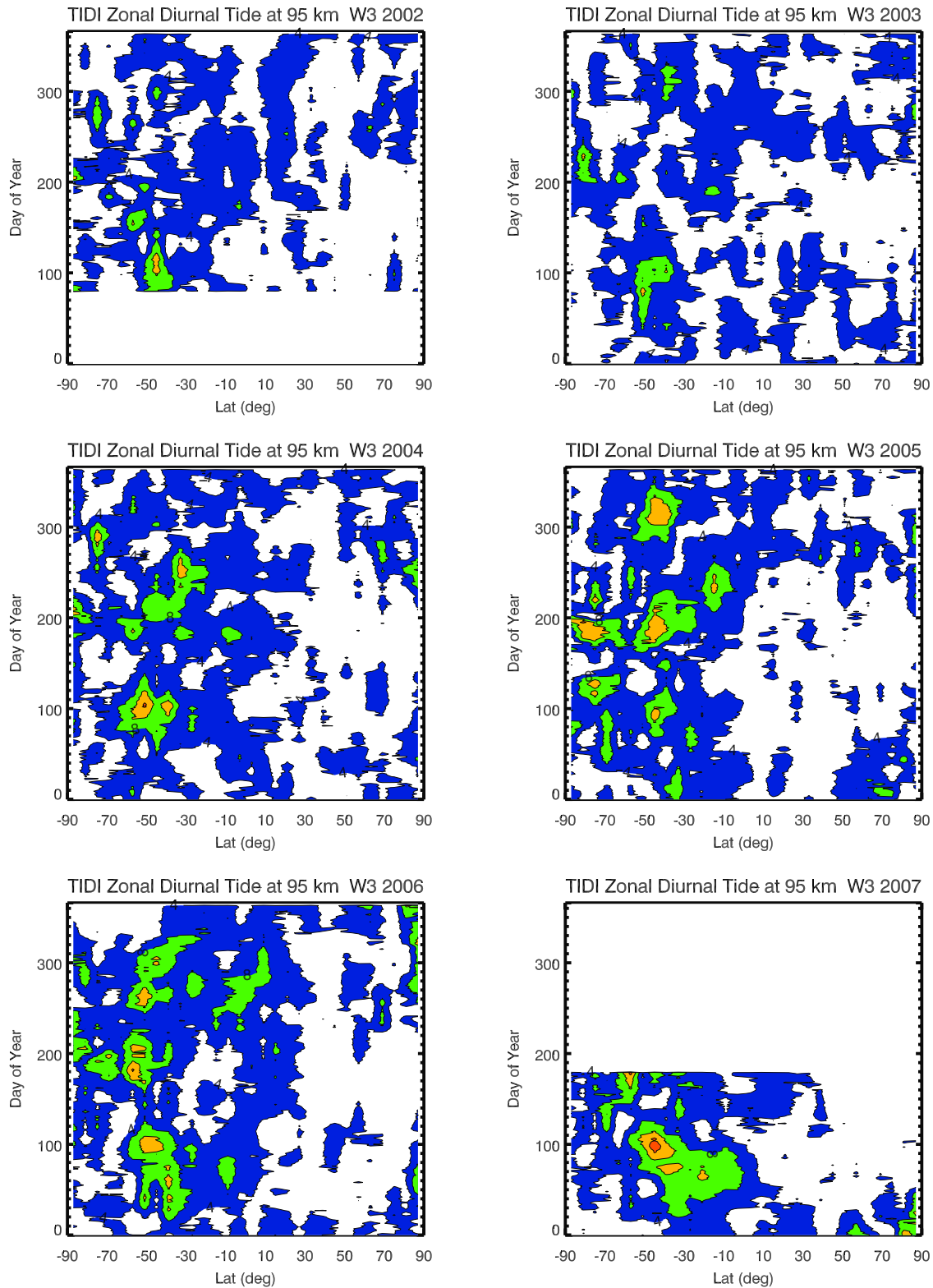


**Figure 21.** Diurnal W3 in zonal winds at 95 km. Same as Figure 1 for W3 in zonal winds.

interaction between planetary wave 1 and migrating diurnal tides; (2) the QBO effect on the peak height was observed during the June solstice on the E3 zonal diurnal tide; (3) several nonmigrating tide components (E3, E2, E1, W3 meridional, and W3 zonal) show similar eastward phase

QBO enhancement during the March equinox, as did the migrating diurnal tide, though to a lesser degree. The QBO effect on some components is less intense during the years of 2006 and 2007.

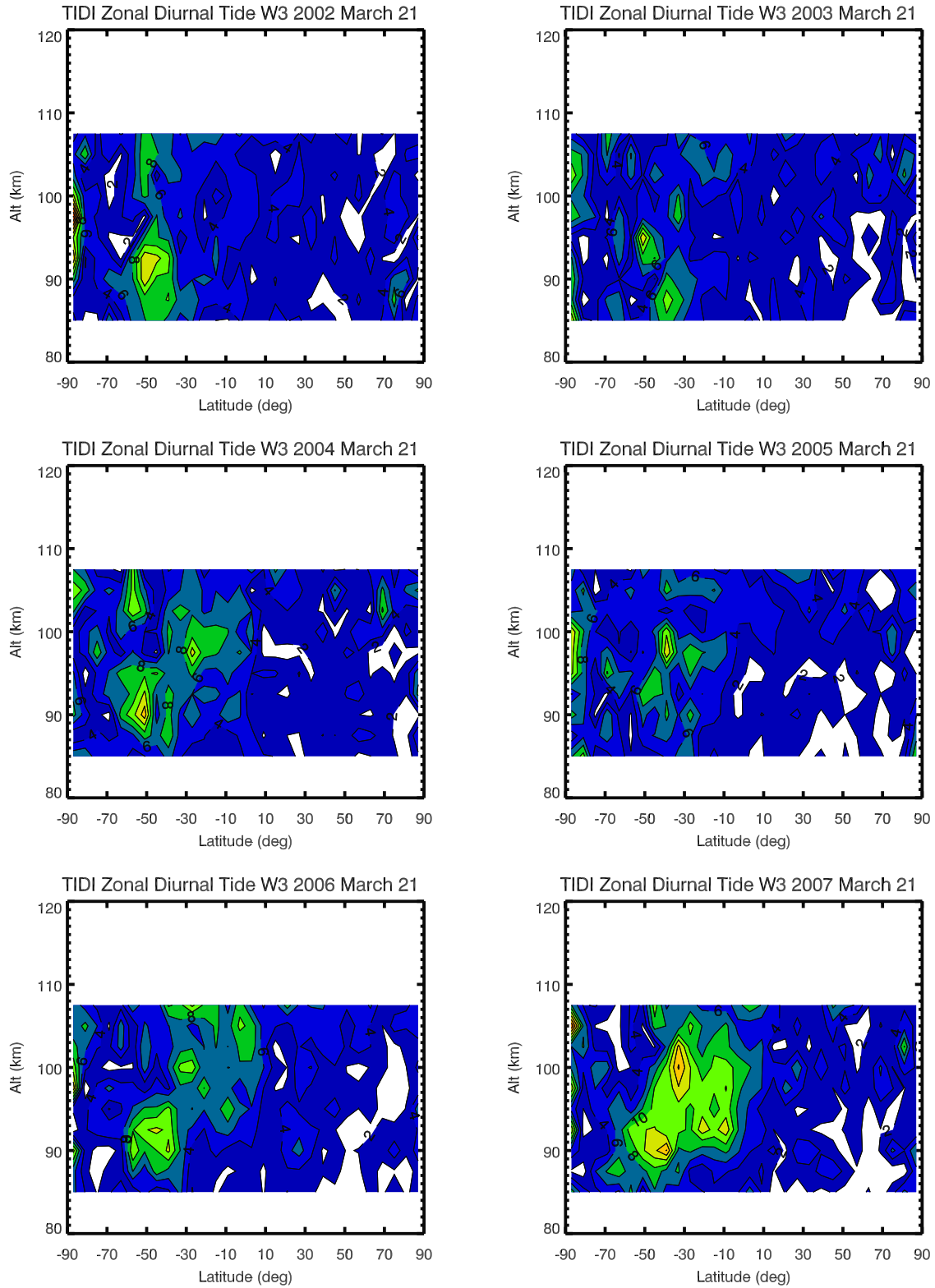


**Figure 22.** Diurnal W3 in zonal winds during the March equinox. Same as Figure 2 for W3 in zonal winds during the March equinox.

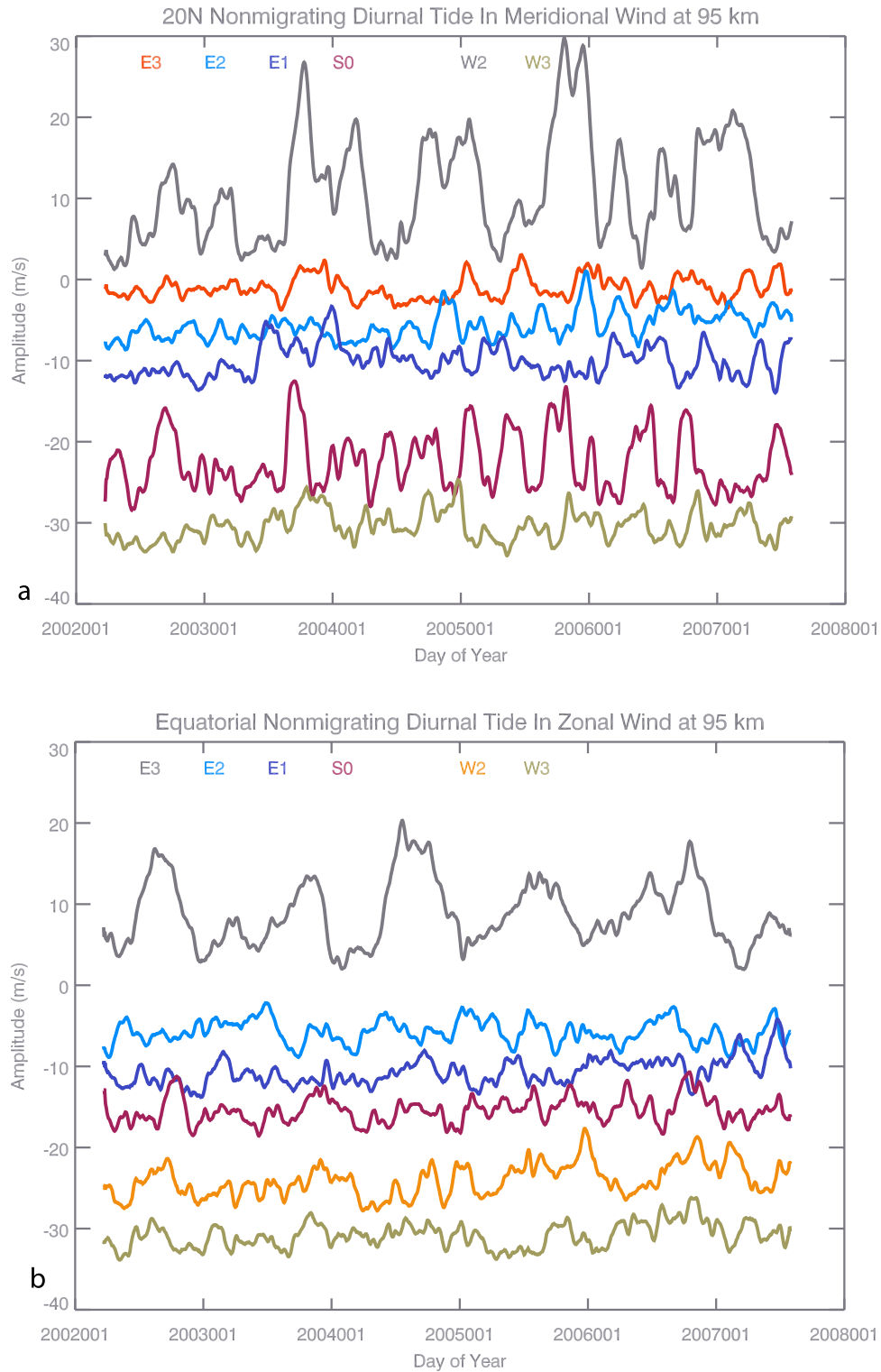


**Figure 23.** Nonmigrating tide temporal variations at 95 km for 20°N (meridional) and the equator (zonal). (a) The meridional wind components at 20°N are displayed. (b) The zonal wind components at the equator are shown. The zero position for each of the components has been shift to display the variation more clearly. Different components are represented in different color as marked in the upper part of each figure.



[27] **Acknowledgments.** This work is supported by a NASA grant NAG5-5334 to National Center for Atmospheric Research and NAG5-5049 to the University of Michigan. NCAR is supported by the National Science Foundation. This work is also supported in part by the Chinese Academy of Sciences International Partnership for Creative Research Teams.

[28] Amitava Bhattacharjee thanks the reviewers for their assistance in evaluating this paper.

## References

- Baumgaertner, A. J. G., M. J. Jarvis, A. J. McDonald, and G. J. Fraser (2006), Observations of the wavenumber 1 and 2 components of the semi-diurnal tide over Antarctica, *J. Atmos. Sol. Terr. Phys.*, **68**(11), 1195–1214, doi:10.1016/j.jastp.2006.03.001.
- England, S. L., S. Maus, T. J. Immel, and S. B. Mende (2006a), Longitudinal variation of the *E* region electric fields caused by atmospheric tides, *Geophys. Res. Lett.*, **33**, L21105, doi:10.1029/2006GL027465.
- England, S. L., T. J. Immel, E. Sagawa, S. B. Henderson, M. E. Hagan, S. B. Mende, H. U. Frey, C. M. Swenson, and L. J. Paxton (2006b), Effect of atmospheric tides on the morphology of the quiet time, postsunset equatorial ionospheric anomaly, *J. Geophys. Res.*, **111**, A10S19, doi:10.1029/2006JA011795.
- Forbes, J. M., N. A. Makarov, and Y. I. Portnyagin (1995), First results from meteor radar at South Pole: A large 12-hour oscillation with zonal wavenumber one, *Geophys. Res. Lett.*, **22**, 3247–3250, doi:10.1029/95GL03370.
- Forbes, J. M., M. E. Hagan, S. Miyahara, Y. Miyoshi, and X. Zhang (2003), Diurnal nonmigrating tides in the tropical lower thermosphere, *Earth Planets Space*, **55**, 419–426.
- Grieger, N., G. Schmitz, and U. Achatz (2004), The dependence of the nonmigrating diurnal tide in the mesosphere and lower thermosphere on stationary planetary wave, *J. Atmos. Sol. Terr. Phys.*, **66**, 733–754, doi:10.1016/j.jastp.2004.01.022.
- Hagan, M. E., and J. M. Forbes (2002), Migrating and nonmigrating diurnal tides in the middle and upper atmosphere excited by tropospheric latent heat release, *J. Geophys. Res.*, **107**(D24), 4754, doi:10.1029/2001JD001236.
- Hagan, M. E., and J. M. Forbes (2003), Migrating and nonmigrating semi-diurnal tides in the upper atmosphere excited by tropospheric latent heat release, *J. Geophys. Res.*, **108**(A2), 1062, doi:10.1029/2002JA009466.
- Hagan, M. E., and R. G. Roble (2001), Modeling the diurnal tidal variability with the National Center for Atmospheric Research thermosphere-ionosphere-mesosphere-electrodynamics general circulation model, *J. Geophys. Res.*, **106**, 24,869–24,882, doi:10.1029/2001JA000057.
- Hagan, M. E., J. M. Forbes, and X. Zhang (2005), *Interannual Variability of Nonmigrating Tides Due to Tropical Latent Heat Release*, IAGA, Toulouse, France.
- Hu, Y., and K. K. Tung (2002), Tropospheric and equatorial influences on planetary-wave amplitude in the stratosphere, *Geophys. Res. Lett.*, **29**(2), 1019, doi:10.1029/2001GL013762.
- Huang, F. T., and C. A. Reber (2004), Nonmigrating semidiurnal and diurnal tides at 95 km based on wind measurements from the High Resolution Imager on UARS, *J. Geophys. Res.*, **109**, D10110, doi:10.1029/2003JD004442.
- Immel, T. J., E. Sagawa, S. L. England, S. B. Henderson, M. E. Hagan, S. B. Mende, H. U. Frey, C. M. Swenson, and L. J. Paxton (2006), Control of equatorial ionospheric morphology by atmospheric tides, *Geophys. Res. Lett.*, **33**, L15108, doi:10.1029/2006GL026161.
- Kato, S., T. Tsuda, and F. Watanabe (1982), Thermal excitation of non-migrating tides, *J. Atmos. Sol. Terr. Phys.*, **44**, 131–146, doi:10.1016/0021-9169(82)90116-7.
- Lieberman, R. S., J. Oberheide, M. E. Hagan, E. E. Remsberg, and L. L. Gordiley (2004), Variability of diurnal tides and planetary waves during November 1978–May 1979, *J. Atmos. Sol. Terr. Phys.*, **66**, 517–528, doi:10.1016/j.jastp.2004.01.006.
- Mayr, H. G., J. G. Mengel, E. R. Talaat, H. S. Porter, and K. L. Chan (2003), Non-migrating diurnal tides generated by planetary waves in the mesosphere, *Geophys. Res. Lett.*, **30**(16), 1832, doi:10.1029/2003GL017877.
- Mayr, H. G., J. G. Mengel, E. R. Talaat, H. S. Porter, and K. L. Chan (2005a), Mesospheric non-migrating tides generated with planetary waves: I. Characteristics, *J. Atmos. Sol. Terr. Phys.*, **67**, 959–980, doi:10.1016/j.jastp.2005.03.002.
- Mayr, H. G., J. G. Mengel, E. R. Talaat, H. S. Porter, and K. L. Chan (2005b), Mesospheric non-migrating tides generated with planetary waves: II. Influence of gravity waves, *J. Atmos. Sol. Terr. Phys.*, **67**, 981–991, doi:10.1016/j.jastp.2005.03.003.
- Murphy, D. J., M. Tsutsumi, D. M. Riggins, G. O. L. Jones, R. A. Vincent, M. E. Hagan, and S. K. Avery (2003), Observations of a nonmigrating component of the semidiurnal tide over Antarctica, *J. Geophys. Res.*, **108**(D8), 4241, doi:10.1029/2002JD003077.
- Oberheide, J., M. E. Hagan, R. G. Roble, and D. Offermann (2002), The sources of nonmigrating tides in the tropical middle atmosphere, *J. Geophys. Res.*, **107**(D21), 4567, doi:10.1029/2002JD002220.
- Oberheide, J., Q. Wu, D. A. Ortland, T. L. Killeen, M. E. Hagan, and R. G. Roble (2005a), Nonmigrating diurnal tides as measured by the TIMED Doppler Interferometer: Preliminary results, *Adv. Space Res.*, **35**(11), 1911–1917, doi:10.1016/j.asr.2005.01.063.
- Oberheide, J., Q. Wu, T. Killeen, M. Hagan, R. Roble, D. Ortland, R. Niciejewski, and W. Skinner (2005b), *Seasonal and Interannual Variability of Nonmigrating Tides in MLT Winds*, IAGA, Toulouse, France.
- Oberheide, J., Q. Wu, T. L. Killeen, M. E. Hagan, and R. G. Roble (2006), Diurnal nonmigrating tides from TIMED Doppler Interferometer wind data: Monthly climatologies and seasonal variations, *J. Geophys. Res.*, **111**, A10S03, doi:10.1029/2005JA011491.
- Sagawa, E., T. J. Immel, H. U. Frey, and S. B. Mende (2005), Longitudinal structure of the equatorial anomaly in the nighttime ionosphere observed by IMAG/FUV, *J. Geophys. Res.*, **110**, A11302, doi:10.1029/2004JA010848.
- Talaat, E. R., and R. S. Lieberman (1999), Nonmigrating diurnal tides in the mesosphere and lower thermosphere winds and temperatures, *J. Atmos. Sci.*, **56**, 4073–4087, doi:10.1175/1520-0469(1999)056<4073:NDTIMA>2.0.CO;2.
- Teitelbaum, H., and F. Vial (1991), On tidal variability induced by nonlinear interaction with planetary waves, *J. Geophys. Res.*, **96**, 14,169–14,178, doi:10.1029/91JA01019.
- Tsuda, T., and S. Kato (1989), Diurnal non-migrating tides excited by a different heating due to land-sea distribution, *J. Meteorol. Soc. Jpn.*, **67**, 43–45.
- Wu, Q., et al. (2008), Global distribution and interannual variations of mesospheric and lower thermospheric neutral wind diurnal tide: 1. Migrating tide, *J. Geophys. Res.*, doi:10.1029/2007JA012542, in press.
- M. E. Hagan, T. L. Killeen, H.-L. Liu, R. G. Roble, S. C. Solomon, and Q. Wu, High Altitude Observatory, National Center for Atmospheric Research, P.O. Box 3000, Boulder, CO 80307-3000, USA.
- R. J. Niciejewski and W. R. Skinner, Space Physics Research Laboratory, University of Michigan, 2455 Hayward Street, Ann Arbor, MI 48109-2143, USA.
- D. A. Ortland, Northwest Research Associates, P. O. Box 3027, Bellevue, WA 98009-3027, USA.
- J. Xu, Key Laboratory for Space Weather, Center for Space Science and Applied Research, Chinese Academy of Sciences, P.O. Box 8701, Beijing, China, 100080.